A SUSTAINABLE AND COST-EFFECTIVE PAVEMENT PRESERVATION METHOD: MICRO-MILLING AND THIN OVERLAY, PERFORMANCE STUDIES WITH 3D SENSING

A Dissertation
Presented to
The Academic Faculty

by

April R. Gadsby

In Partial Fulfillment
of the Requirements for the Degree
Master of Science in the
School of Civil and Environmental Engineering

Georgia Institute of Technology
December 2017

A SUSTAINABLE AND COST-EFFECTIVE PAVEMENT PRESERVATION METHOD: MICRO-MILLING AND THIN OVERLAY, PERFORMANCE STUDIES WITH 3D SENSING

Approved by:

Dr. Yi-Chang Tsai, Advisor
School of Civil and Environmental Engineering
Georgia Institute of Technology

Dr. James Lai
School of Civil and Environmental Engineering
Georgia Institute of Technology

Dr. Zhaohua Wang
Center for Geographic Information Systems
Georgia Institute of Technology

Date Approved: November 14, 2017

ACKNOWLEDGEMENTS

First, I'd like to thank Dr. Tsai for his support and guidance over the years. He has helped me grow immensely over the three years we have been working together. In particular, he has helped me develop my critical thinking and communication skills, which will aid me throughout my life. I am also very grateful for all the opportunities he has given me, including presenting at TRB as an undergraduate, presenting at a global conference in Seoul, South Korea, and a plethora of scholarship and award opportunities, many of which I won due to his support. He has taken great care to consider how to improve my career opportunities, and I am finishing my degree as a much more confident and effective researcher and, in general, a better, well-rounded person.

I also want to thank others in the lab. I especially want to thank Yi-Ching Wu, Ross Wang, and Georgene Geary for their mentoring. They have all contributed greatly to my growth and success. However, I could not have accomplished all I have in this lab group without the aid and camaraderie of the other members of the group, including Lauren, Cibi, Geoffrey, Anirban, Nora, Yifei, Dr. Wang, Dr. Ai, Vincent, Segolene, and many others who were here for a short time over the last three years. Furthermore, I would like to thank my many other mentors who may not have been in the lab group but had an impact on my time as a student. Many people, too numerous to list here, have touched my life in a positive way since I came to Georgia Tech, and I am thankful to have met all of them.

Finally, I'd like to thank my family and friends (especially Casey Smith and Katie Horton) for their unwavering love and support.

TABLE OF CONTENTS

LIST OF TABLES

LIST OF FIGURES

LIST OF SYMBOLS AND ABBREVIATIONS

AADT	Annual Average Daily Traffic
AADTT	Annual Average Daily Truck Traffic
ASCE	American Society of Civil Engineers
CRCP	Continuously Reinforced Concrete Pavement
CSV	Comma Separated Values
CTM	Circular Track Meter
EIO-LCA	Economic Input Output Life Cycle Assessment
EUAC	Equivalent Uniform Annual Cost
FETA	Faulting Evaluation and Texture Analysis
GaTech	Georgia Tech
GDOT	Georgia Department of Transportation
GPS	Global Positioning System
GTSV	Georgia Tech Sensing Vehicle
GWP	Global Warming Potential
HCS IRI	Half Car Simulated International Roughness Index
HMA	Hot Mix Asphalt
HTP	Human Toxicity Potential
IMU	Inertial Measurement Unit
IRI	International Roughness Index
JPCP	Jointed Plain Concrete Pavement
LCA	Life Cycle Assessment
LCCA	Life Cycle Cost Analysis

LCMS	Laser Crack Measurement System
LiDAR	Light Detection and Range
MPD	Mean Profile Depth
MTD	Mean Texture Depth
NPV	Net Present Value
OGFC	Open Graded Friction Course
PACES	PAvement Condition Evaluation System
PaLATE	Pavement Life cycle Assessment Tool for Economic and Environmental Effects
PCC	Portland Cement Concrete
PEM	Porous European Mix
RAP	Reclaimed Asphalt Pavement
RVD	Ridge-to-Valley Depth
SMA	Stone Matrix Asphalt
VMT	Vehicle Miles Traveled

SUMMARY

Micro-milling and thin overlay is a pavement preservation treatment in which a thin, worn-out top layer of pavement is removed and replaced, leaving the underlying sound layers largely untouched. The benefits and costs of this treatment had been largely unquantified, so there was a need to quantify the effectiveness and sustainability of the treatment. The objective of this thesis became the remedy to this situation: to quantify the performance of micro-milling and thin overlay and improve rapid 3D data collection for the quality control measure that would aid decision-makers in their efforts to choose and implement the most effective and sustainable pavement treatments for their roadways.

Performance was measured on three of the first micro-milling and thin overlay projects in Georgia using a combination of Georgia Department of Transportation (GDOT) manual survey data and 3D sensing data. The results showed the treatment has an estimated service interval of 10-12 years, the same as that of conventional milling, and that it may be an effective crack relief treatment. Where safety is a concern and money is lacking, micro-milling may be used to abate rutting for up to 4 years.

After determining that the treatment performed well, the sustainability assessment could begin. The cost-effectiveness was studied using life cycle cost analysis and considered the construction and material costs. The results showed that micro-milling and thin overlay could save Georgia over $500 million per year on its interstate system if it were used instead of conventional milling. The life cycle assessment using the PaLATE spreadsheet showed that micro-milling reduced energy usage by 61.9%, a reduced water usage by 61.8%, and reduced CO_2 emissions by 61.7% over conventional milling,

primarily due to reduction in materials use. The social benefits were mainly attributed to increased construction timing flexibility and reduced construction time, which reduced exposure of drivers and workers to dangers associated with interstate construction. This sustainability analysis shows micro-milling and thin overlay to be a more sustainable pavement preservation option than conventional milling and overlay.

In addition to the sustainability assessment, the quality control measure, ridge-to-valley depth (RVD), needed an improved code for automatic processing using 3D sensing technologies. The code was modified to ensure the calculation matched reality as closely as possible and to automatically process a series of images. This code was used to assess the adequacy of the current standard for RVD. Based on initial assessment, it was concluded that RVD does not impact crack propagation. Currently, raveling is minimal on the assessed section of I-95, so it seems the measurement is effective, but whether it can be relaxed will need to be considered when the pavement is older.

The contributions of this thesis, summarized here, fill in knowledge gaps that had previously existed about this new pavement preservation treatment. The quantifications will aid decision-makers in Georgia and other states decide whether or not micro-milling is a viable option for their agency or project and the outlined RVD measurement method using 3D sensing can help them perform quality control on the treatment. Based on the improved cost-effectiveness, environmental impacts, and social sustainability, it can be recommended that this treatment be considered by more agencies and a national specification be designed to support it, which the information contained within this thesis can aid in.

CHAPTER 1.   INTRODUCTION

In 1956 President Eisenhower signed the Federal Aid Highway Act of 1956, and the US Interstate Highway System began to be built, but there was little concern for future maintenance. Vehicle miles traveled (VMT) has grown considerably since 1956, increasing from just over 1 trillion miles per year in 1971 to just over 3 trillion miles per year in 2007; since then, the growth has levelled off (*1*). This tripling of VMT has encouraged the building of more and bigger infrastructure, which now must be maintained. As the signing of MAP-21 (*2*) in 2012 and the FAST Act (*3*) in 2015 has shown, as VMT increase slows, pavement deteriorates, and budgets are spread thinner, focus has shifted to preserving pavements rather than building more. VMT is expected to increase at a rate of only 0.78% annually from 2015-2045, which considers the decrease in passenger traffic and increase in light duty vehicles, based on *FHWA Forecasts of Vehicle Miles Traveled: Spring 2017* (*4*). But, the most recent ASCE report card has given America's roads a D, calling them "chronically underfunded" (*5*). According to the report, 20% of the nation's highways were in poor condition in 2014, which costs motorists $112 billion/year in extra vehicle repairs and operating costs (*5*). Overall, there is a need of $836 billion in repairs and capital investment for America's highway system (*5*). Therefore, transportation agencies are looking to cost-effectively maintain their roads to create high-quality and sustainable roadway systems.

The Georgia Department of Transportation (GDOT) recognized the need to maintain its deteriorating pavements despite a limited budget, so, in 2007, GDOT decided to test a new pavement preservation technique involving micro-milling a thin open graded wearing

course and replacing it with a thin overlay of an open graded wearing course. Micro-milling has been used by other agencies to address their pavement maintenance needs. GDOT was the first to use micro-milling with a thin overlay of an open graded wearing course.

1.1 Micro-Milling in the United States

To begin a discussion of micro-milling, it is necessary to define micro-milling. Micro-milling is sometimes called fine milling or, more infrequently, surface planing (*6*). There is a distinction between fine milling and micro-milling. Micro-milling uses a drum with 5 mm bit spacing, which is three times the number of bits on a conventional milling drum, whereas fine milling has 8 mm bit spacing, which is approximately twice the number of bits on a conventional drum (*7*). However, these are often used interchangeably, making it difficult to distinguish the two when looking at their use across the country. An effort was made to distinguish between agencies using micro-milling from those using fine milling, but this was not always possible. Georgia uses micro-milling with the 5-mm bit spacing.

Evidence was found that 19 states are using micro-milling; however, few are using it for the same purpose as Georgia. Generally, micro-milling is used for improving skid resistance, restoring a road's profile, or for milling and overlaying operations with varying overlay thicknesses. The most common quality control measure used is the glass bead test, but a different one is used in Georgia and will be discussed in the next section. As an example of a state that uses micro-milling in a manner similar to Georgia, Massachusetts uses micro-milling to mill and apply a thin leveling course that it follows with an open-graded friction course (*8*). An interesting change is that Massachusetts takes advantage of

the flexible construction to open the milled surface to traffic through the winter and overlays in the spring to avoid the extra patching and traffic control costs caused by the winter weather (*8*). Massachusetts isn't the only state that leaves the micro-milled surface open to traffic. Typically, states that use micro-milling for improving skid resistance leave the surface open to traffic, a use similar to diamond grinding use on concrete. Some states that use micro-milling for this purpose include Michigan, Nevada, and Ohio (*9*). Georgia, among other states, uses micro-milling to address concerns such as raveling on the surface layer, but some states use it to remove minor rutting, such as Nebraska (*10*), and some states, such as California, use it to remove other pavement deformation problems (*11*). New York mills and replaces a removed layer with a layer of a different thickness (*8*). Only a handful of states have implemented micro-milling as a major part of their roadway maintenance strategy, but states such as Massachusetts, Rhode Island, and Washington have used it extensively (*8*, *12*). However, in 2013, FHWA published a report concerning how pavement treatments impact roadway safety and determined that micro-milling was not widely used enough to consider it in their report (*13*). Overall, micro-milling is still fairly new, but it is growing in popularity. Thus far, the only scholarly articles regarding micro-milling of asphalt pavements have been published by Georgia DOT and Georgia Tech, all of which will be discussed in the following section.

1.2 Micro-Milling and Thin Overlay in Georgia

The typical GDOT interstate pavement design is shown in Figure 1-1. The surface layer is a thin open graded wearing course, either open graded friction course (OGFC) or porous European mix (PEM). OGFC and PEM are very similar, but PEM has a higher air void content (18-22% as compared to 15% for OGFC) and PEM is more gap graded, and

thus more permeable, than OGFC (*14*). These layers allow water to drain through them and out between the surface layer and the stone matrix asphalt (SMA) layer, reducing splash and spray and improving visibility and safety in rain. The SMA is a gap-graded mix with a high number of coarse aggregates that create an interlocking matrix that is stronger than in a typical dense graded pavement. This SMA layer can still be sound when the OGFC layer fails after 10-12 years (*15*). It is important to note that OGFC is used in Georgia on all interstates paved with asphalt pavement, but it can also be used on state roads with high traffic. The design for the state routes is not shown because they are highly traffic dependent, and this thesis focuses on interstates. However, the findings can be applied to state routes in most cases.

7/8" OGFC or 1.25" PEM	XXXXXXXXXXXXXX
1.5" SMA	/ / / / / /
2" Asphaltic Concrete B 19mm	
4" Asphaltic Concrete Base 25 mm	
10" Graded Aggregate Base	
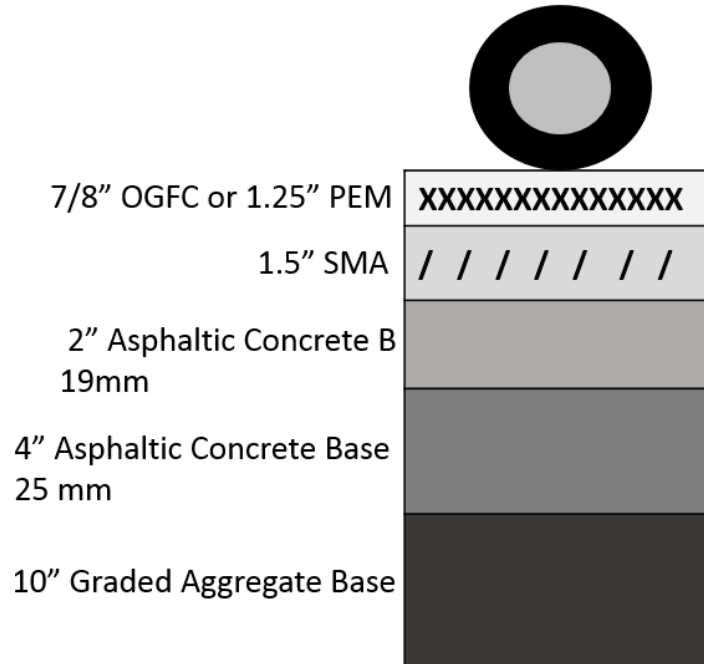
Figure 1-1 – Typical GDOT interstate pavement design with "X" marking the layers removed by both micro-milling and conventional milling and "/ / /" marking the layer removed by conventional milling only

Conventional milling and overlay removes both the OGFC and SMA layers after the OGFC fails, which means that about half of the life of the SMA is lost in this process. However, concerns about water entrapment due to the flow of water between the porous and SMA layers during rain leading to delamination led GDOT to choose conventional milling as standard practice (*15*). In 2007, GDOT decided to challenge this standard practice by using micro-milling and thin overlay to preserve the remaining life of the SMA, which appeared to be both a financially and environmentally beneficial decision. However, many innovations and changes were needed to ensure that this method would be successful, including a new quality control specification, a measurement tool for the specified measurement, and new construction practices.

The developments in this pavement preservation technique were primarily made during the first two micro-milling projects. The first project occurred in 2007 on I-75 south of Macon, Georgia, on 15.3 miles with 3 lanes in each direction for a total of 91.8 lane miles. This section had an average annual daily traffic (AADT) of approximately 50,100 vehicles and 25% truck traffic (*17*). It was constructed in 1969 and resurfaced in 1997. In 2005, the pavement condition evaluation showed that the top layer had deteriorated with visible raveling and load cracking (*15*). After testing cores with an asphalt pavement analyzer, it was determined that the underlying layer, a dense-graded hot mix asphalt (HMA) pavement, was still sound. To delay a full depth repair and thus save money (approximately $4.7 million on this project), a micro-milling and thin overlay process was devised. The project commenced in 2007 with micro milling and a PEM overlay.

Based on the success of the I-75 project, micro-milling was again chosen to preserve the pavement on I-95 near Savannah, Georgia. This project was 14 miles long with 3 lanes in each direction, or 84 lane-miles. It was last widened and resurfaced in 1995. The top layer was OGFC with an underlying 1.5" layer of SMA. In 2007, the pavement condition evaluation showed severe raveling and some longitudinal and transverse cracking. After testing cores with an asphalt pavement analyzer, it was determined that the SMA was still in good condition and construction commenced in 2010 and, due to weather concerns, finished in 2011. This project had an estimated cost savings of $5.7 million.

1.2.1   *Development of the RVD Measurement*

Conventional milling uses a drum with wider, larger teeth and a larger separation between teeth than the drum used for micro-milling, which uses many small, tightly-spaced

6

teeth. These smaller, more tightly-spaced teeth create a smoother surface after milling and reduces water entrapment between layers. However, even with micro-milling, water entrapment was still a concern, so a new construction quality measurement was devised: ridge to valley depth (RVD). This measures the difference between the highest and lowest points in a pavement over a specified distance, typically 100 mm, as shown in Figure 1-2. Many papers and reports have been published in regards to this measurement (*18–21*).
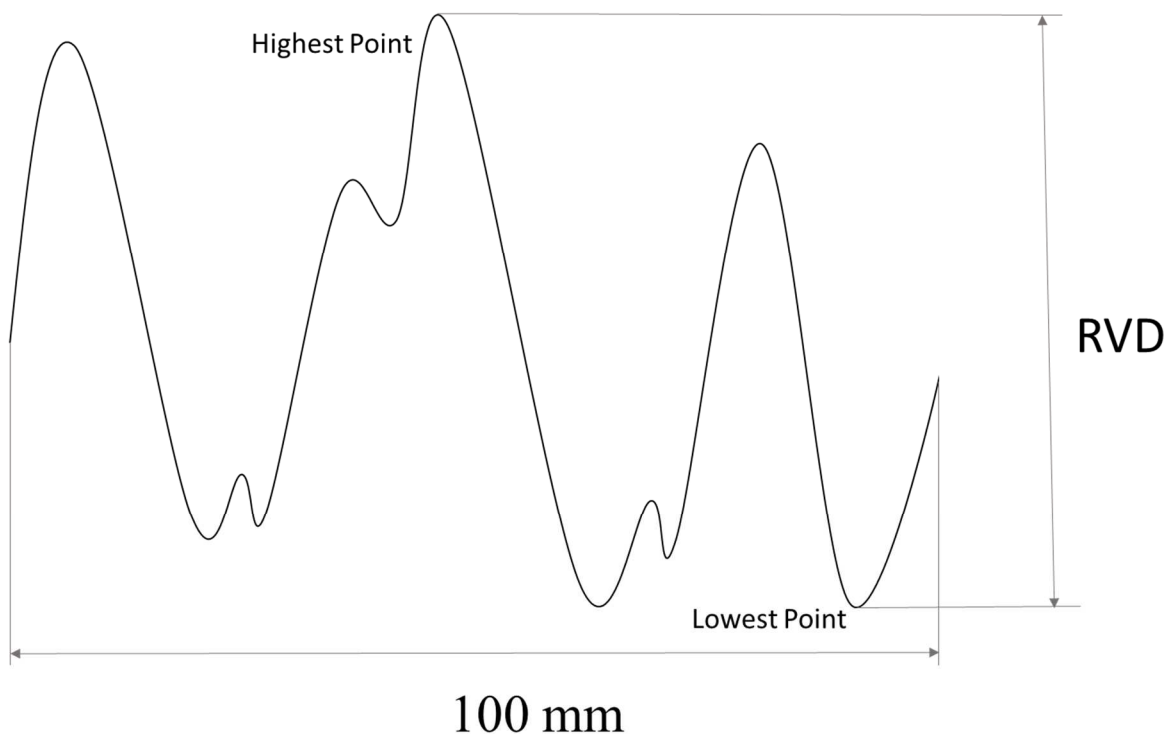
Figure 1-2 – Simplified Demonstration of RVD Computation

RVD was initially developed by James Lai to reflect the need to reduce potential water entrapment (*19*). The measurement was compared to mean texture depth (MTD) and mean profile depth (MPD) to determine the correlations and the possibility of converting one value to another. It was found that the relationship between MTD or MPD and RVD

is dependent on the macrotexture characteristics, which can be symmetrical, negative symmetrical, or positive symmetrical; however, these characteristics are not easily determined (*18*). Therefore, RVD must be directly measured, which is possible with a retrofitted laser road profiler such as was used for GDOT's first micro-milling project. Later, it was determined that RVD could be measured using 3D sensing technology (*19*).

As with any measurement, a threshold was needed to give meaning to the measurement. A threshold of 1.6 mm Mean RVD for compliance and 3.2 mm p95 RVD for corrective actions were chosen based on discussion with statisticians and pavement engineers (*18*). They also recommended that P95 be used over p90 after analysis of measurements from the first micro-milling project. The analysis determined that p90 and p95 were quite close, so the more rigid option, p95, was chosen as the requirement (*18*). On the next micro-milling project, however, the p95 RVD of 3.2mm was too difficult to meet, and the requirement was relaxed to a mean of 3.2mm after some further research to determine if this could be acceptable. It was determined to be acceptable based on a good 3-year performance (*20*).

A further study by Tsai et al. (*19*) looked at the statistical distributions of RVD on smooth and rough segments. This research further demonstrated that a mean RVD of 3.2mm is adequate to differentiate between a rough and a smooth segment. This research showed that rough segments follow an approximately normal distribution, and smooth segments follow a similar distribution but with a substantial positive skew in comparison to a rough section (*21*). This research reassessed the original 100 mm base length set for measuring the RVD, which was chosen to be consistent with ASTM E1845(*22*) for calculating MPD.

In the initial analysis, it was determined (based on circular track meter (CTM) results on the initial micro-milling project) that maximum surface texture depths are higher when they are either perpendicular or diagonal to the milling direction (*18*). Laser road profilers only work in the parallel direction to the milling direction, which would have meant that to get the highest measured values, a CTM may have been necessary. However, work by Tsai et al. showed that it is possible to measure full-lane coverage RVD using 3D sensing technology (*19*). Using the full lane enables the identification of isolated spots of poor macrotexture. The 3D sensing process further allows for measuring the RVD in any direction. The transverse direction was chosen because it best represents the path of water runoff (*19*). A long-term study confirming these assessments, particularly the 3.2 mm Mean RVD for corrective actions, is still needed and will be addressed in Chapter 5.

1.2.2   Construction Practices

Construction practices employed also impact the long-term performance of the thin overlay. These have been refined as projects were performed and are described in Tsai et al. (*23*). Pre-treatments are performed prior to construction. For sections showing damage to the layers deeper than the micro-milling depth, deep patching is performed. The I-95 project distresses requiring deep patching included high severity load cracking and raveling (*23*). This operation consisted of milling 2 inches deep, placing a 3/8 inch mat to prevent any crack propagation, and then repaving with SMA (*23*). Prior to full commencement of the micro-milling operation, a 1,000-ft test section is micro-milled to ensure that the micro-milled surface conforms to the requirements specified in GDOT Special Provision Section 432 (*24*). If the section fails, as it did in both the I-75 and I-95 projects, then the contractor will submit a plan that must be approved by the GDOT engineer to adjust the operation,

such as adjusting milling speed and drum speed, to meet the requirements (*23*). A second test section is then micro-milled and assessed, and the failed section is re-milled. Once appropriate settings are chosen, the micro-milling operation can commence.

The surface is frequently checked to ensure the operation is still meeting requirements; the average RVD is measured every ½ mile. On the I-75 project, a 7/8-in micro-milling was specified in the contract, but it was discovered through the course of construction that this depth could not guarantee full removal of the OGFC, especially approaching bridges, so the specification was changed to variable depth micro-milling for the rest of the project and future projects. It was also determined that a combination of appropriate milling machine speed, cutting drum speed, teeth pattern, and underlying material is needed to produce a smooth micro-milled surface. On the I-95 project, the material was sticking to the teeth, leading to a poor surface, which was addressed by adding a soap solution to the water spray to clean the milling drum. Additionally, worn-out micro-milling teeth were causing poor results, which was addressed by replacing the worn out teeth on a daily basis. (*23*)

It was also discovered on the I-95 project, the first on SMA, that due to the large coarse aggregate in the SMA, some large aggregates were being dislodged, creating pockets in the surface and increasing the RVD. To check for this, a clean surface is necessary. A clean surface is also necessary for adequate bonding of the binder. A power broomer was used to clear the smaller particles produced in the micro-milling process; it had to be operated more slowly than after conventional milling. The micro-milled surface is very smooth after cleaning, so it can be left open to traffic. GDOT allows this for up to 5 days, if needed, providing flexibility to the contractor. The traffic allows dust on the

surface left after the broom operation to be blown out, cleaning the surface further. However, the ridges can be smoothed due to loading, so the number of days the surface can be exposed to traffic needs to be limited for accurate RVD measurement. (*23*)

Quality control of this pavement was performed using GDOT's laser road profiler for both projects. The I-95 project was the first to explore the use of full-coverage measurement of the micro-milled surface using 3D sensing technology, which can be used for future projects (*23*).

After the cleaning and quality control is complete, the paving operation can commence. First, a tack coat is applied to the freshly cleaned surface. Based on experimental tests on the I-75 project, a tack coat application rate of 0.08 gal/yd^2 is recommended. Following tack coat application, the open graded wearing layer is placed on top and compacted using a rubber roller. The paved surface is tested for acceptance using GDOT's laser road profiler to measure the Half Car Simulated International Roughness Index (HCS IRI), which must meet a target value of 825 mm/km and not exceed 900 mm/km. Further study based on the long-term performance of these construction practices is still needed. This thesis will assess the long term performance of the projects and begin assessing whether pretreatment may be needed for cracking on the milled surface and what existing pre-conditions qualify a project for micro-milling. (*23*)

1.2.3 Sustainability

With long-term data, an assessment of the overall sustainability of the practice can be accomplished. Sustainability is typically modeled as a 3-legged stool. The three legs of the stool are environmental, social, and economic sustainability. These exist within the

context of a location/society that can be considered the ground. Altogether, when balanced, these hold up a sustainable society. There is much debate about the definition of sustainability. For this report, the ASCE definition of sustainability will be used: "a set of economic, environmental, and social conditions in which all of society has the capacity and opportunity to maintain and improve its quality of life indefinitely without degrading the quantity, quality, or the availability of economic, environmental, and social resources" (*25*). In terms of pavement maintenance, sustainability can focus on all three aspects.

The sustainability analysis of micro-milling and thin overlay was begun by Tsai et al. (*15*). It assessed the performance of the pavement after micro-milling on the I-75 project and the economic sustainability through a life cycle cost assessment. The findings showed that a micro-milled and thin overlaid pavement has an approximate service interval of 10-11 years, comparable to that of conventional milling, which is 10-12 years. Also, the analysis showed that micro-milling and thin overlay can, conservatively, save $27,000 per lane-mile. However, this study can be expanded with more performance data and with more recent cost data to reflect more up-to-date micro-milling costs. An introduction to the process of assessing the environmental sustainability of micro-milling and thin overlay was presented at the MAIREINFRA conference in 2017 (*26*). A more complete life cycle assessment is included here with a section discussing the social sustainability.

1.3 Objectives

The objectives of this thesis are to analyze the long-term performance of micro-milling and thin overlay, perform a more complete sustainability assessment, refine a code to

calculate RVD, and develop a procedure to critically assess the RVD specification initially set.

1.4   3D Sensing

Before discussing this project further, 3D sensing used in this thesis must be described and defined. The Georgia Tech Sensing Vehicle (GTSV) was used to collect the sensing data mentioned in this thesis (unless specified otherwise). The GTSV is sponsored by the United States Department of Transportation and is equipped with emerging technologies, including 2D imaging, 3D laser imaging (laser crack measurement system (LCMS)), 3D light detection and range (LiDAR), a global positioning system (GPS), and an inertial measurement unit (IMU). The integration of these sensors can be used for a variety of tasks, such as creating 3D images of the pavement. Resolution of the acquired road surface data is approximately 1 mm in the transverse direction and 5mm in the longitudinal direction. The measurement accuracy is 0.5 mm in the elevation direction. Images of the sensing van are shown in Figure 1-3. These technologies combined will be called "3D sensing" throughout the thesis.

Figure 1-3 – Georgia Tech Sensing Vehicle

1.5 Thesis Organization

This thesis is organized as follows: Chapter 1 introduced micro-milling and thin overlay and outlined the motivation and objectives of the thesis. Chapter 2 analyzes the performance of the micro-milling and thin overlay method. Chapters 3 and 4 assess the economic, environmental, and social sustainability of the method. Chapter 5 discusses automation of the RVD calculation and assesses the current specification. Chapter 6 summarizes conclusions and presents recommendations for future work.

CHAPTER 2.   PERFORMANCE ANALYSIS

Fundamentally, no pavement preservation treatment can be implemented if it does not perform well. As mentioned in Chapter 1, the first micro-milling project has been in service for 10 years. With this long-term data, it is possible to study the long-term performance of this pavement preservation treatment. This chapter will consider three of the early micro-milling and thin overlay projects: I-75, completed in 2007; I-95, completed in 2012; and I-285, completed in 2012. The three projects will be analyzed from three different perspectives. The I-75 project occurred prior to the existence of the GTSV, so GDOT performance data will be used for the assessment. This data is aggregated on the mile and project level, so it can provide a high-level view of the pavement performance. For the I-95 project, 3D sensing data is available on the micro-milled surface, so a detailed analysis of the precondition of the pavement and how it performed over time is possible. In particular, it is possible to assess the location and timing of which types of cracks reflect. I-285 has no precondition data, but it was in poor condition when micro-milling and thin overlay was applied due to money concerns (*16*). This makes I-285 of interest for assessing how the pre-condition impacts performance. I-285 has 3D sensing data after the micro-milling available, and the cracking and raveling can be assessed.

2.1   Project Descriptions

The first project considered is on I-75 just south of Macon, Georgia. It had an AADT of 50,100 with 25% trucks in 2007, and despite a decrease in the following years, has returned to an AADT of 50,200 with 25% trucks in 2016. It is 3 lanes in each direction, and the

project 15.3 miles long, making it 91.8 lane-miles. The I-75 project location, lane configuration and traffic are shown in

Figure 2-1 (A). The pavement design is shown in Figure 2-2a. This pavement has an older mix, Asphaltic Concrete E, instead of SMA, and PEM as the open graded surface layer.

The I-75 pavement section was originally constructed in 1964 using jointed plain concrete pavement (JPCP). It was overlaid with asphaltic concrete in 1994, and micromilling and thin overlay was performed in 2007. Figure 2-2 shows the existing pavement design. This design has been in service for 10 years now and has not yet needed replacement. Initial expectations for this project, due to the newness, were that it would last 3-4 years (*15*), but it has lasted as long as a conventional milling and overlay project.

The second project considered is on I-95 near Savannah, Georgia. The project on I-95 was approximately 14 miles long with 3 lanes in each direction (84 lane-miles). Construction began in 2011 and, due to weather concerns, finished in 2012. It had an AADT of 67,810 in 2011, which has grown to 84,500 in 2016, as shown in

Figure 2-1. The truck percentage is around 14%, resulting in approximately 11,000 trucks per day in 2016, about 1000 less per day than I-75.

Figure 2-1b shows the location of the project, lane configuration, and traffic counts since 2011.

This section was originally constructed in 1971 using 8.5" continuously reinforced concrete pavement with a 6" pre-mixed soil cement sub base. However, the pavement has

since been topped by asphaltic concrete, as shown in Figure 2-2b. The OGFC layer is from the thin overlay, replacing an older open graded surface layer, asphaltic concrete D mod, which is no longer used. This design has been in service for 6 years now with only a few miles showing cracking.
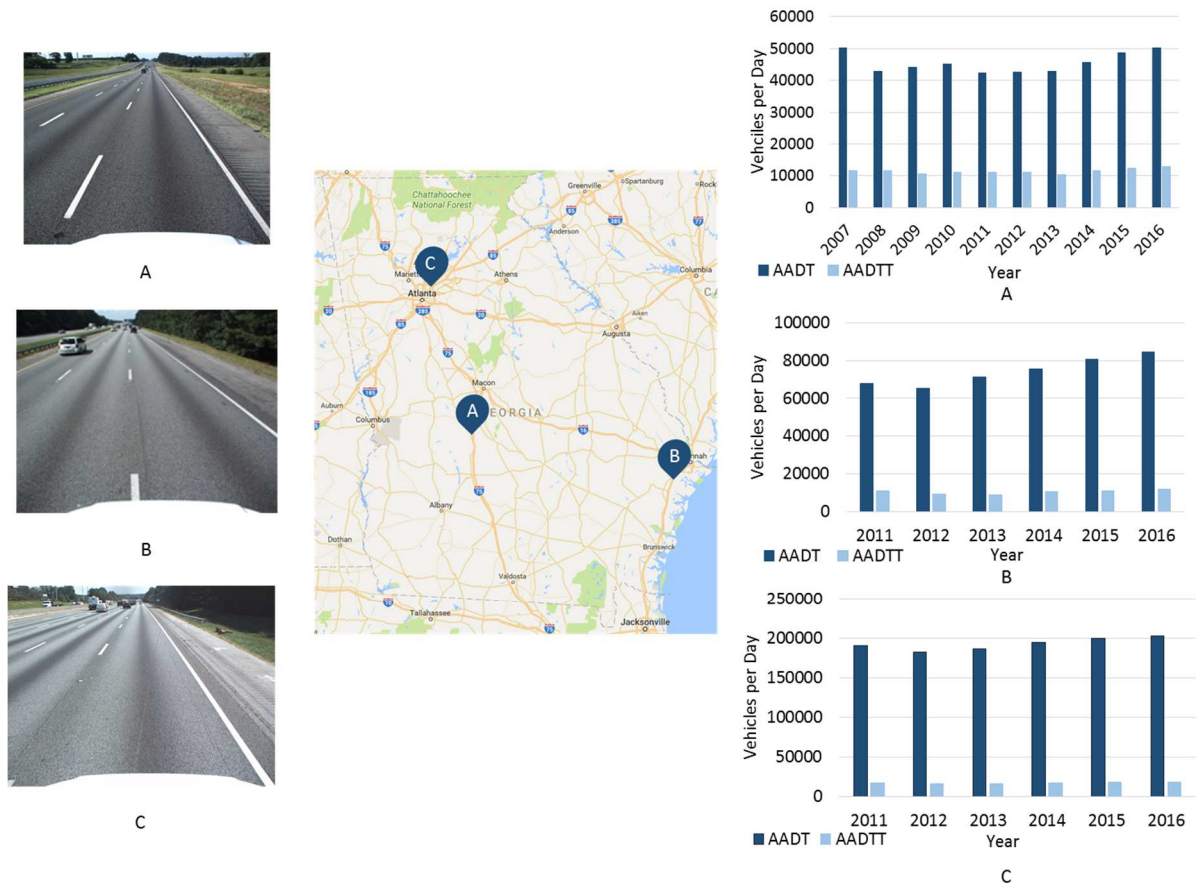
Figure 2-1 – Project location, lane configuration, and traffic on I-75 (A), I-95 (B), and I-285 (C)

I-75

1.25" 12.5 mm Porous European Mix

1.5" Asphaltic Concrete E

2" Asphaltic Concrete B

4" Asphaltic Concrete Base

10" JPCP with 3" Bituminous Stabilizer and 5" Granular Sub-base

I-95

7/8" Open Graded Friction Course

1.5" Fine Stone Matrix Asphalt

2" Asphaltic Concrete B

8.5" CRCP with 6" Soil Cement Sub-base

(a) I-75   **(b) I-95**
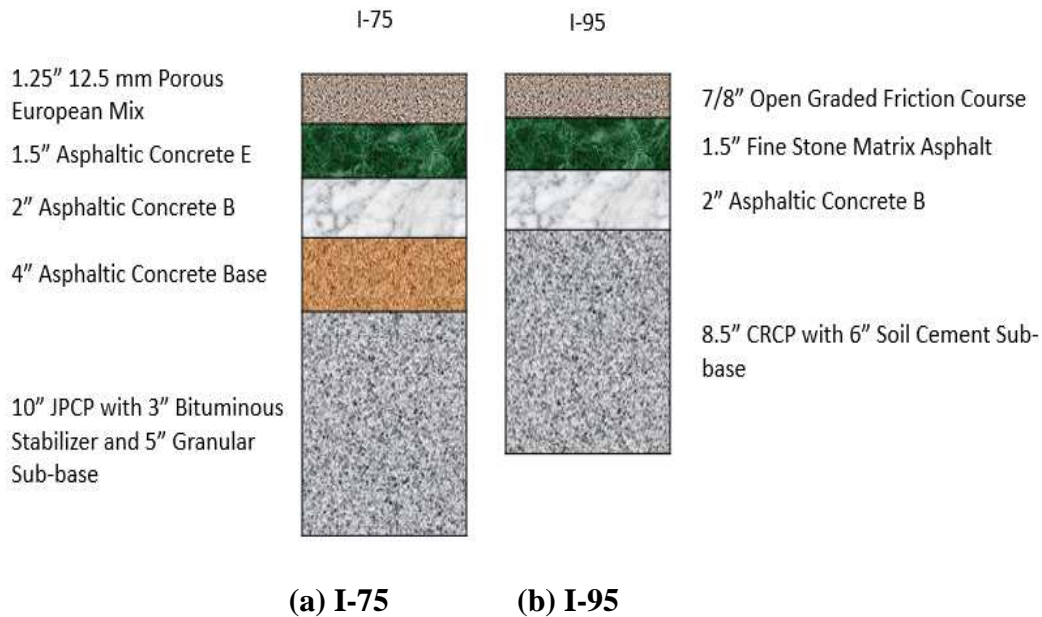
Figure 2-2 – Pavement structure on I-75 and I-95

Less information was available for the I-285 section. I-285 is an interstate that goes around Atlanta, and this project took place on the north east part of it. The project was completed in 2012. It is approximately 6.6 miles long, and the number of lanes varied during the project with a minimum of 3 lanes in each direction. It had an AADT of approximately 200,000 VPD with 8% truck traffic, as shown in

Figure 2-1(C) . Half of the section has underlying Portland cement concrete (PCC) overlaid with hot mix asphalt pavement. The other half is full-depth asphalt pavement with a 1.5" Asphaltic Concrete E layer under the PEM, similar to the pavement design on I-75. PEM was the overlaid layer for this project.

2.2   Performance studies

The following sections will assess the performance of each of the three projects.

18

2.2.1   I-75

The performance on I-75 will be assessed using GDOT's Pavement Condition Evaluation System (PACES) data (*27*). PACES evaluates pavement condition and assesses 10 types of pavement distresses. Each pavement distress is rated by severity and extent. Most distresses have three levels of severity; Severity Level 1 represents low severity, and Severity Level 3 represents high severity. These ratings are converted to an overall rating on a scale of 0 to 100, with 100 being a perfect pavement and 70 being the cutoff for an acceptable pavement. This data is given on the project level, typically 7-10 miles, and the segment level, typically 1 mile. Cracking is assessed in a representative 100-foot segment where detailed measurements are taken, and most other distresses are assessed over the entire mile using a windshield survey.

Prior to micro-milling and thin overlay on this section of I-75, the pavement was in poor condition, indicated by its PACES rating of 65 (out of 100). The poor rating was primarily attributable to raveling, reflective cracking, and some load cracking. There was extensive Severity Level 2 reflective cracking, which means that all joints had reflected, and the cracks were wide enough that they could require sealing. Unfortunately, there are two types of transverse cracking in PACES: block and reflective cracking. Without prior knowledge of the roadway construction, it is easy for raters to mistake reflective cracking as block cracking. Prior to 2007, it was often recorded as block cracking, and this was the case in 2006, so the 2005 ratings had to be used. In 2005, there were 148 feet of Severity Level 2 reflective cracking. There was also extensive Severity Level 1 raveling with 93%

of the section raveled in 2006. There was also some minor load cracking first recorded in 2006.

Nine years after the overlay, the project is still in fair condition, having a PACES rating of 77 in 2016. The 2016 rating was created using an algorithm developed in-house that calculates PACES ratings based on the 3D sensing data. Although the results seem reasonable after looking at images of the pavement, they may be lower than the results of a manual survey because 3D automatic detection of raveling tends to detect raveling earlier than the human eye. Figure 2-3 shows the project's PACES rating by age before and after milling with the years 1994 and 2007 as age 0. PACES is a manual rating system that can produce some inconsistencies, and the PACES survey is not performed in some years, so there may be gaps in the data; however, PACES data was the only data available for this thesis project. Despite the gaps, the PACES data is strong enough to support this thesis project's analysis. Although the ratings appear to be very similar before and after construction, some differences can be attributed to the different surface layers and construction. In 1994, full-depth reconstruction was performed, which means a surface layer was laid on a perfect asphalt pavement, whereas the surface layer after micro-milling was laid on an asphalt pavement layer that was already 14 years old. The 1994 pavement had an older design, called asphaltic concrete D, but this was replaced with porous European mix in 2007. The mixes were of different design and had the same purpose, but the performance, especially raveling, could have been impacted by the different mixes.
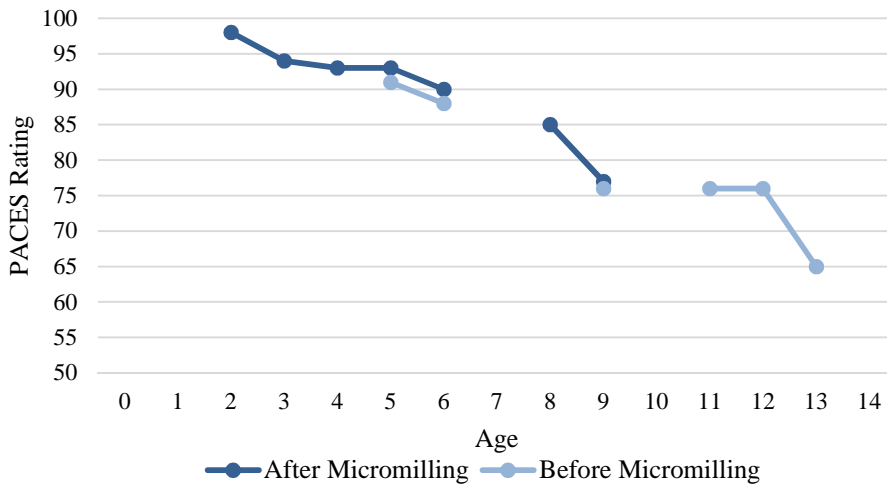
Figure 2-3 – Project rating comparison before and after micro-milling and thin overlay

Figure 2-4 shows the raveling and reflective cracking extent before and after micro-milling by age. As previously mentioned, the reflective cracking prior to micro-milling was often recorded as block cracking, which is measured using a different type of extent, so it was excluded from this graph. Transverse cracking of any kind was first recorded in 1999, which is at age five. This was also the first year that a survey was performed. Reflective cracking started on the post micro-milling surface at age four, so the reflective cracking began at similar ages before and after. Raveling began for both at age six. It progressed rapidly, but the year nine data from the post micro-milling are from the automated PACES data, which, as discussed, tends to detect raveling earlier than manual rating.
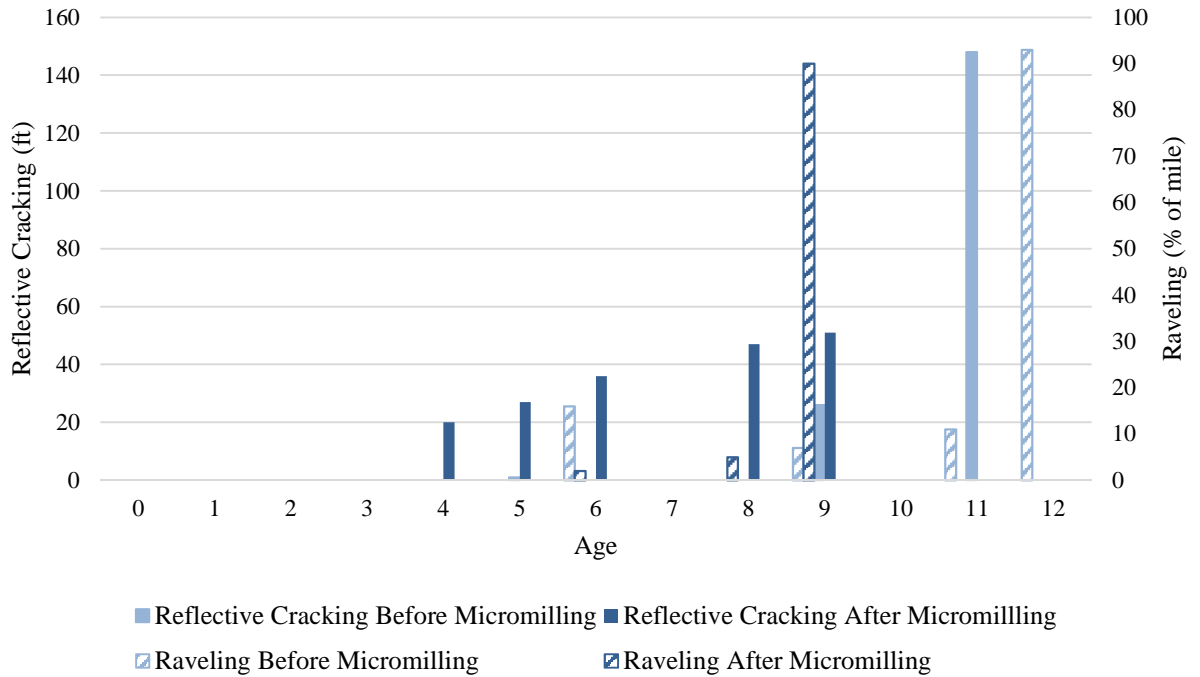
Figure 2-4 – Project level reflective cracking and raveling before and after micro-milling

Based on the pavement performance on the I-75 project and the similarity in performance before and after micro-milling, an approximate service interval of 10-12 years can be concluded. This is higher than the 10-11 year service interval found in 2016, which was adjusted to accommodate the current state of the pavement and the added knowledge of the before and after conditions from this assessment (*15*).

2.2.2 I-95

A PACES survey is performed using manual inspection methods; most cracks are assessed on a selected 100' section that is supposed to be a representative section for the mile. This is a subjective measurement method. PACES also analyzes distresses in a lump sum approach, so it is impossible to determine if an individual crack has reflected from the

underlying surface or is new. However, 3D sensing methods can solve these problems. This section will demonstrate another way of assessing the impacts of the pre-condition of a micro-milled surface and the propagation of cracks following overlay by using 3D sensing data to accurately measure the cracks. Since I-95 was the first micro-milling and thin overlay project to have 3D sensing technology used in it, it is the best candidate for a longer-term analysis.

For this thesis analysis, one mile was chosen so that a detailed assessment of the cracks could be performed to utilize the strength of the 3D sensing technology. Using PACES data as an overview, MP 96-95 in the southbound direction was chosen because it had the most cracking recorded. After selecting the mile for detailed analysis, a beginning and ending point had to be chosen that could be seen in the 3D images of the road both immediately after milling and in 2016. The chosen section, given this constraint, begins just after the Mile 96 marker and continues until the exit at Mile 94, making the distance longer than 1 mile (approximately 1.5 miles). Once the beginning and ending points are identified, cracks are detected using an in-house program that can measure the length and width of cracks. Next, the images and crack maps are manipulated to allow for a visualization that aligns the images so that cracks can be matched to assess which cracks are propagated or if the crack is new. With the aligned cracks, an analysis of the cracks can be performed.

There were 2,005 feet of cracking with an average width of 0.6 inches on the section in 2011 on the milled surface. Table 2-1 shows the cracking by type and year. As can be seen in Table 2-1, the majority of these cracks were transverse cracks, but some longitudinal cracks were present. Longitudinal cracking is separated into non-wheelpath

and wheelpath because the wheelpath cracking is assumed to be caused by traffic loading, whereas non-wheelpath is caused by weathering and aging.

Table 2-1 – Comparison of Total Crack Length

Year	Crack Length (ft.)			
	Transverse	**Non-wheel-path Longitudinal**	**Wheel-path Longitudinal**	**Subtotal**
2011	1,556	331	118	2,005
2013	0	0	0	0
2014	22	1	0	23
2015	45	6	0	51
2016	94	32	28	154

A selection of cracks to demonstrate the diversity of cracking on the mile is shown in Figure 2-5. The range images are on the right. These images show depth, which can make the cracks easier to see. Each range image covers five meters. These images were used for the crack detection. Many cracks were thin, such as the first in Figure 2-5's series of images, but some were wider, as shown in the bottom image in Figure 2-5, and many had wide sections near the right side. However, the width of the cracks did not impact the crack propagation. The third image shows an especially bad crack and the only cracking to

propagate prior to a construction joint located approximately ½ mile (850 meters) into the section.
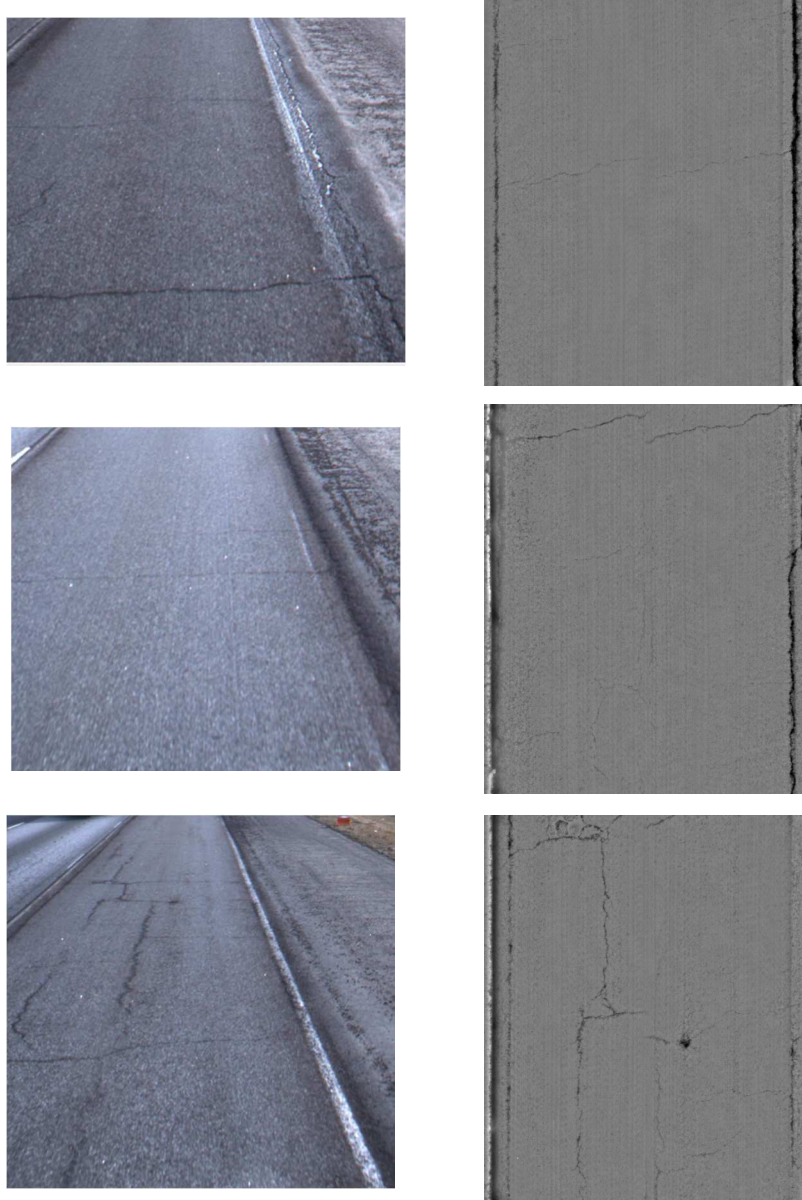
Figure 2-5 – Videolog images and 3D sensing data on milled surface in 2011

Table 2-2 can also be used to consider the amount of cracking on the surface in years 2013, 2014, 2015, and 2016. Cracking did not start until 2014, 2 years after completion of the overlay. Load cracking started 4 years after completion of the overlay in

2016. Considering the total cracking, there is only 154 feet of cracking in 2016 compared to the 2,005 feet in 2011. However, the overall cracking does not show which cracks are propagated and which are new. Table 2-2 shows the cracking by type in 2011 and 2016, and it shows how much has propagated onto the surface in 2016 and how much new cracking formed in 2016. Of the 2,005 feet of cracking on the milled surface, 106 feet of cracking propagated. An additional 48 feet of new cracking appeared. The most common type of cracking to propagate was the transverse cracking with 94 feet of transverse cracking propagated and 12 feet of longitudinal cracking. The longitudinal cracking was located in an especially severe area of cracking, shown in the bottom image of Figure 2-5.

Table 2-2 – Crack propagation using registered crack maps

	Cracks in 2011			Cracks in 2016		
	Subtotal	**Reflected in 2016**	**Non-reflected in 2016**	**Subtotal**	**Reflected from 2011**	**Non-reflected from 2011**
Transverse	1,556	94 (6%)	1462 (94%)	94	94 (100%)	0 (0%)
Non-wheel-path Longitudinal	331	12 (4%)	319 (96%)	32	12 (37%)	20 (63%)
Wheel-path Longitudinal	118	0 (0%)	118(100%)	28	0 (0%)	28 (100%)
Subtotal	2,005	106 (5%)	1900 (95%)	154	106 (69%)	48 (31%)

Spatially, the 2016 cracks are clustered in the latter half of the section. Figure 2-6a and b show the cracking distribution by number of cracks and by length of cracks, respectively, aggregated into 10m segments. Figure 2-6b has the longitudinal cracking length removed, as those did not propagate and tend to be longer than transverse cracks. As can be seen in Figure 2-6, no cracks reflected in the approximately first 850 meters of the section. The latter section is the only one with cracking on the whole project, and nearly all of the cracking is after a construction joint. Therefore, it is assumed that the difference in performance can be attributed to differences in construction.
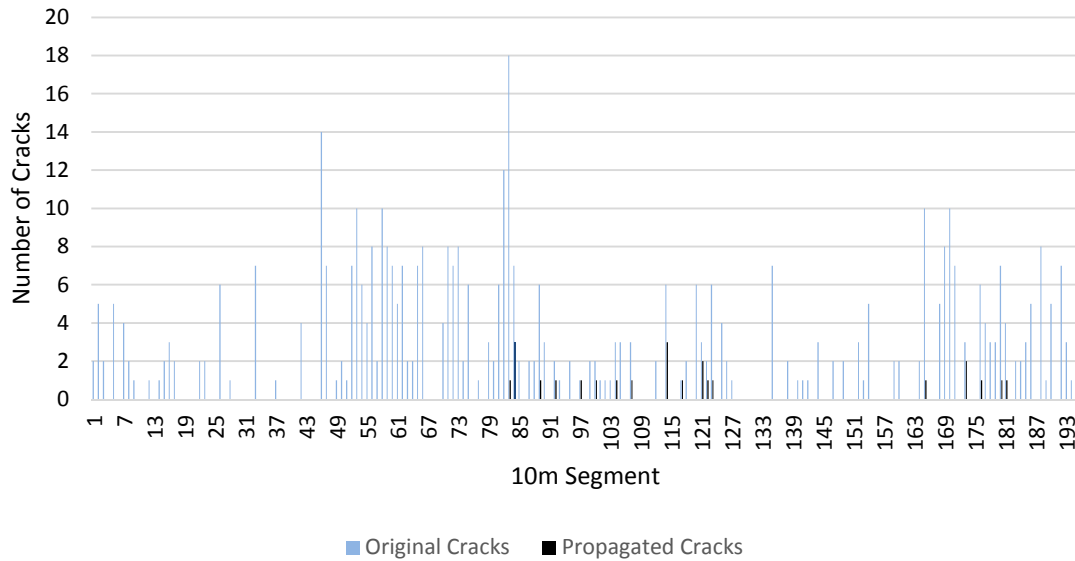
(a) Count by Number
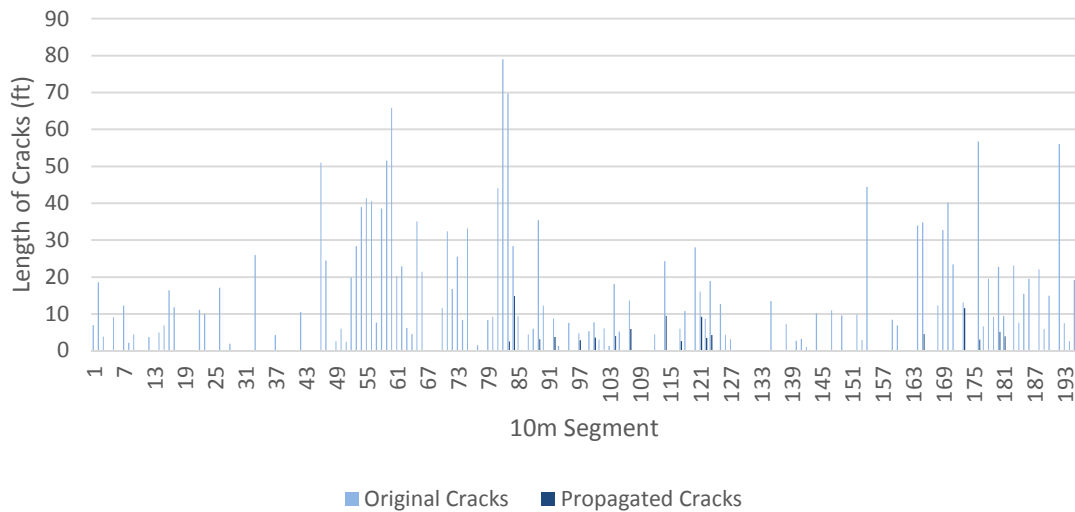
(b) Count by Length

Figure 2-6 – Spatial distribution of cracks in 2011 and reflected cracks in 2016

With 3D sensing methods, it is possible to track individual cracks. Because the increase in crack length is attributed to both lengthening of individual cracks and

appearance of new cracks, it is of interest to follow a selection of cracks to observe their propagation characteristics. Three cracks that had clear images each year were chosen. Their range images from 2014, 2015, and 2016 are shown in Figure 2-7. It can also be seen in Figure 2-7 that the transverse cracks typically start from the right side of the lane and lengthen towards the left. The increasing crack length and width can be visually seen here, and the length increase is numerically shown in Table 2-3. The percent change (marked as Delta) is given in Table 2-3, as well. The rate of change varies between cracks and from year to year.
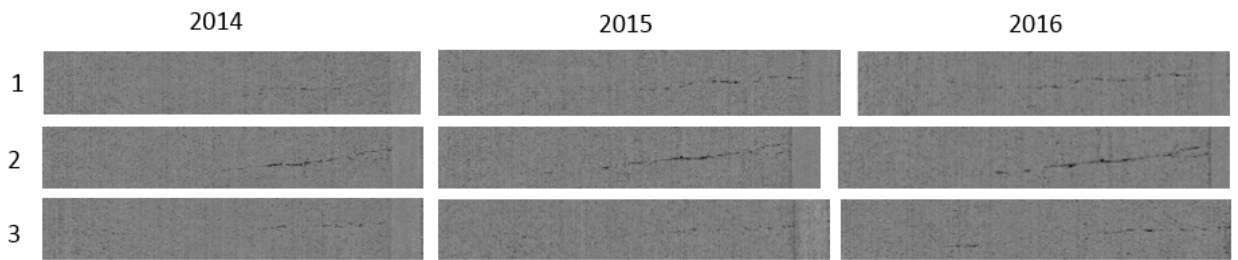
Figure 2-7 – Propagation of three individual cracks

Table 2-3 – Detailed crack length and change for 3 cracks

	Crack 1		Crack 2		Crack 3	
Year	Length (ft.)	Delta	Length (ft.)	Delta	Length (ft.)	Delta
2014	1.94	--	3.63	--	2.52	--
2015	2.89	49%	3.92	8%	2.99	19%
2016	3.77	31%	4.64	18%	4.53	51%

Based on this analysis, reflective cracking is the biggest concern, in particular transverse reflective cracking. The width and length of the crack on the milled surface did not have an impact on whether or not a crack propagated. Furthermore, load cracking did not propagate by 2016, and there was some new load cracking, suggesting that load cracking may be a form of top down cracking. Overall, little cracking has propagated to the surface (just 5%), suggesting that OGFC is a good crack relief layer and that the pre-condition on I-95 was more than sufficient for micro-milling and thin overlay to succeed.

2.2.3   I-285

No PACES data is available for I-285, so the routinely collected 3D sensing data is used for this analysis, as well. No precondition survey was performed for I-285, so only the performance after micro-milling is possible to assess. 3D sensing data was available for this section for 2013, one year after completion of the micro-milling, to 2017. Both cracking and rutting was observed for this section. After a visual inspection, a section in the clockwise direction from exit 30 to 31A was chosen for analysis. This is approximately 1 ¾ miles long. Although no record was available of the pre-existing condition on I-285, people who were involved with the project or who work for GDOT state that the condition on I-285 was poor, potentially lacking structural integrity for micro-milling and thin overlay, as shown by rutting (*16*, *28*). Micro-milling was used anyway due to a lack of money at the time and a need to remove rutting that was causing safety concerns. This initial poor condition on I-285 is why I-285 is of interest. This project can show how effective micro-milling is on a pavement in poor condition and help differentiate between good and bad candidates for micro-milling and thin overlay.

The cracking on I-285 looks to be reflective cracking from the underlying PCC. Near the beginning of the section, the old off-ramp can be seen reflected, as shown in the first row of images in Figure 2-8. Figure 2-8 shows a selection of cracking images from the assessed section in 2013 (left) and 2017 (right). The second image shows a reflected construction joint that runs near the wheelpath; the positioning likely is causing more rapid deterioration. This cracking runs throughout most of the project and accounts for most of the longitudinal cracking. Many of the transverse cracks also appear to be reflected joints. The bottom images in Figure 2-8 show the most extreme example of this. Based on a visual assessment, it seems the cracking problems on I-285 can be attributed to reflective cracking.
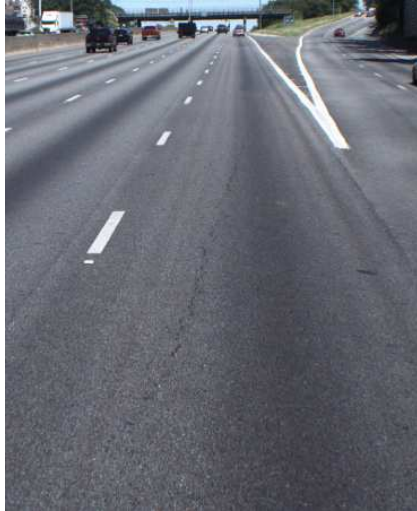
Figure 2-8 – Examples of cracking on I-285 in 2013 (left) and 2017 (right)

Cracking initiated earlier in this project than the I-95 project. On I-285 cracking was already appearing by 2013 and extended 351 feet, which is more than double the

cracking in 2016 on I-95. The cracking grew more rapidly, as well, increasing by 2,481 feet of cracking between 2013 and 2017, 7 times the amount of cracking in 2013. The I-95 results showed that the open graded surface layer may act as a good crack relief layer, but the cracking appeared more rapidly on I-285. This could be attributed to the higher traffic loading or the condition of the road prior to micro-milling, which suggested a weakening of structural support in some of the deeper layers.

Because rutting was the original concern on this thesis project, it is necessary to consider it here. An in-house rutting code was used to find the mean, maximum, and spatial distribution of the rutting on I-285. The average and maximum rutting for the left and right wheelpaths is shown in Table 2-4. The rutting is calculated every 2 feet, and these statistics were found across the entire analysis section from each 2-foot reading. On average, the rutting across years remained at approximately 1/10 inch. This is not a concerning level of rutting, but the maximum rutting beginning in year 2014 is approximately ½ inch, which is a high level of rutting. The rutting decreases in some years, which could be due to maintenance activities or inaccuracies in the data or code. Because the maximum is high, but the average is acceptable, the location of the high rutting needed to be considered to see how long the sections of high rutting lasted.

Table 2-4 – Rutting mean and maximum for the left and right wheelpaths by year in eighths of an inch

	Mean (1/8")		Maximum (1/8")	
	Left	Right	Left	Right
2013	0.5	1.2	1.5	3.3
2014	0.8	1.2	1.9	3.8
2015	0.8	0.8	2.2	3.6
2016	0.9	0.8	2.2	3.6
2017	0.9	1.4	2.6	4.2

For the spatial distribution analysis, the rutting was averaged per 5m image, previously measured at one rutting value taken per foot.

Figure 2-9a and b show the rutting in eighths of an inch per image in 2017. Aggregated at the image level, the maximum rutting is approximately 2.3 and 1.3 eigths of an inch for the right and left wheelpaths, respectively. This is still within an acceptable range, although the right wheelpath is somewhat high. It can futher be shown that the highest rutting does tend to occur in groups, which means it could be reduced by patching operations, but there are many of these clumps, so this may not be as effective as desired. This is especially true in the left wheelpath, which has more uniform rutting throughout the section. Looking at the rutting aggregated in this way, it can be concluded that micro-milling and thin overlay can ameliorate rutting for five or more years as the rutting on a 5m basis has not exceeded an acceptable value. However, due to the randomly distributed 1/2" of rutting in 2017, it is suggested the use of rutting amelioration on poor roads be limited to 4 years.
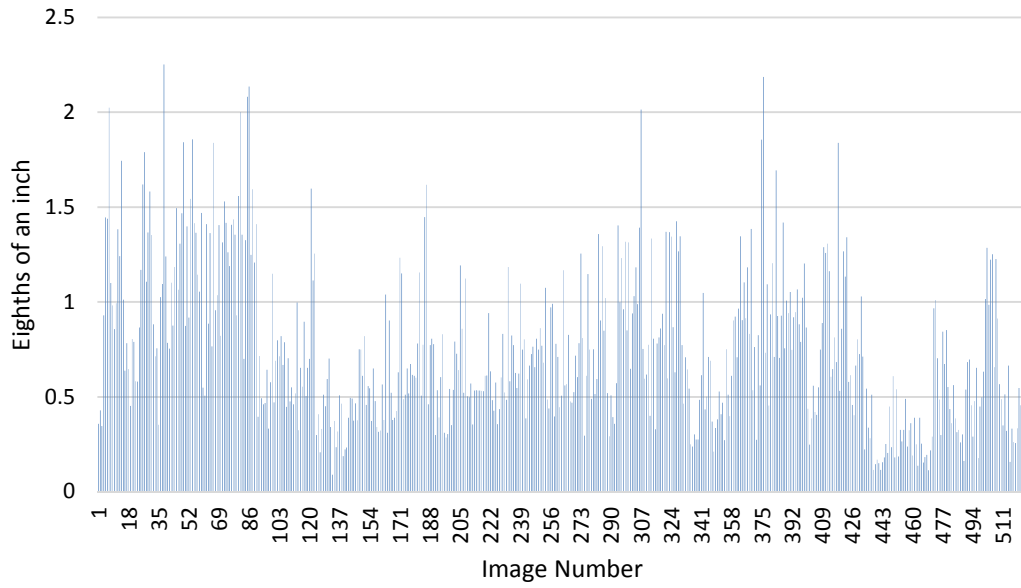
(a)
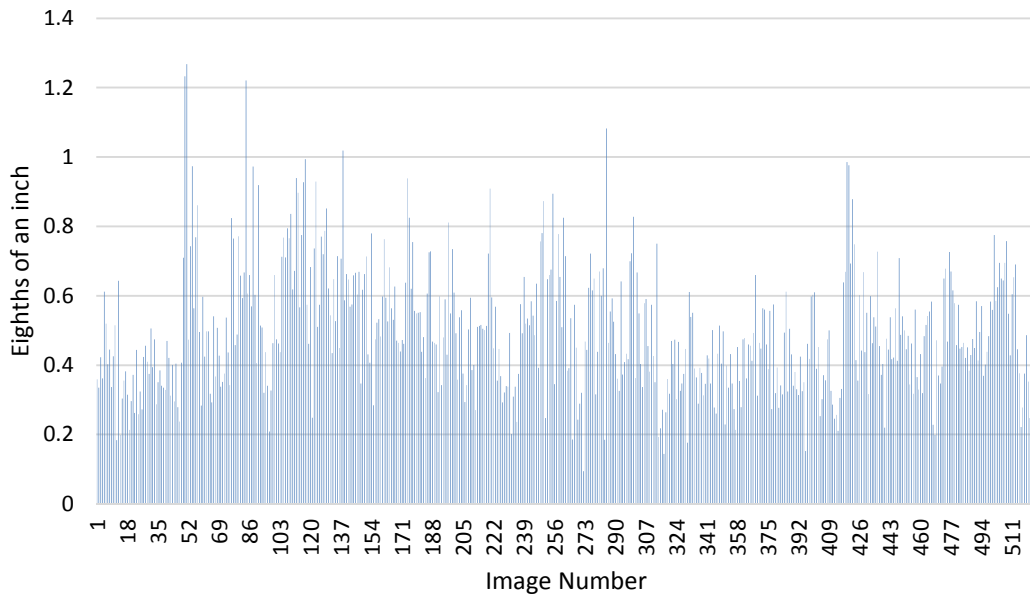
(b)

Figure 2-9 – Spatial distribution of rutting in the right (a) and left (b) wheelpaths

2.3   Summary

Based on these analyses, micro-milling and thin overlay is shown to be an effective pavement preservation treatment. From the first micro-milling project, it has been shown that micro-milling can last 10 years, as this project has, and that micro-milling has an expected service interval of 10-12 years. The I-95 project further supported this with its pavement condition after 5 years of service. The I-95 analysis focused on cracking and reflection of cracks through the overlay. This analysis showed that only minor amounts of cracking had reflected through (5% of the original cracking), suggesting this is an effective crack relief method. The I-285 project was considered because of the original poor condition of the pavement. The reflective cracking did progress more quickly than on I-95, but that could be related to traffic loading or the severity of the original condition. The micro-milling did ameliorate the rutting temporarily (for approximately 4 years), so it can be used as a temporary treatment for rutting.

With the performance assessment showing that micro-milling and thin overlay is an effective treatment for a worn out top layer, crack relief, and temporary rut abatement, the next step is to consider the cost-effectiveness in assessing the overall effectiveness and sustainability of micro-milling and thin overlay.

CHAPTER 3.   ECONOMIC SUSTAINABILITY

Life cycle cost analysis (LCCA) is a method of assessing and comparing project costs over a lifetime, including materials, construction, maintenance, and end-of-life. In deciding whether to use micro-milling and thin overlay or conventional milling, the cost is of primary concern, so an LCCA is of interest. An LCCA for micro-milling was previously done by Tsai et al. (15). This study used 8 years of pavement performance data to look at the I-75 project and develop an expected service interval for micro-milling and thin overlay. The service interval, based on the condition of the pavement and engineering judgement, was approximated to be 10-11 years. This value was then used in an LCCA to determine the cost-effectiveness of micro-milling and thin overlay and compare it to conventional milling and overlay. This LCCA included material and construction costs only, assuming all other costs were the same for the two treatments. It concluded that micro-milling can save 11% over conventional milling.

There were some limitations to this study that will be addressed in this chapter. The first is that no micro-milling project had reached the given service interval. As detailed in Chapter 2, the I-75 project is now 10 years old and still in service with a PACES rating of 77. This means it may exceed the expected service interval, so an adjusted service interval of 10-12 years will be used here, which is the same interval used for conventional milling. Another limitation is that the cost data did not come from a specific project but was aggregated data from a different year than the I-75 project. As micro-milling was a new process, the costs would be expected to be higher. Updated costs from a real project using both treatments will be used for the milling in this updated LCCA.

3.1 I-95 Project Description

This LCCA will use data from a recent micro-milling project on I-95 extending from I-16 to the Savannah River near South Carolina. The project is 13 miles long and 3 lanes in each direction for a total of 78 lane-miles. The segment had an AADT of 84,500 vehicles in 2016 with 14% trucks. The top two layers of the new pavement are 1.5" SMA and 7/8" OGFC. The project was originally let as a micro-milling and thin overlay project, but due to concerns of rutting, was changed to conventional milling on the 2 outside lanes and micro-milling on the inside lane. This means there are 52 lane-miles of conventional milling and 26 lane-miles of micro-milling. The conventional milling was completed during summer 2017, and the micro-milling and OGFC overlay has yet to be completed. For this thesis, the contractor for the project was contacted, and more detailed information about the project was obtained. This information will be used in both this chapter and Chapter 4.

3.2 Life Cycle Cost Assessment

The rest of this chapter will consist of a description of the LCCA inputs and an analysis of the results, a sensitivity study, and conclusions.

3.2.1 Inputs/Parameters and Results

The service interval used in this LCCA is 12 years for both the micro-milling and the conventional milling. This is chosen because both have an approximate service interval of 10-12 years, and a sensitivity study will be performed to assess sensitivity to the service interval. A discount rate of 4% is used, which is within the recommended range by FHWA

and GDOT (*2*). The unit of study is a 12-foot wide lane for 1 lane-mile. The costs include the materials (SMA and OGFC) and construction costs (micro-milling and conventional milling). The costs are aggregated to include the construction, equipment, and labor. The costs for the milling were obtained from the I-95 project contractor, which improves the comparison because they are from the same project. The material costs (SMA and OGFC) were obtained from the most recent item mean summary (*3*) using the weighted average cost for 12.5 mm OGFC and SMA 12.5.

Costs in addition to materials and construction were considered. The two treatments being assessed are pavement preservation treatments themselves, so there are no other maintenance costs. User costs were considered, as overall production of micro-milling and thin overlay can progress more quickly than conventional milling, but it was decided that they would not be included in this analysis. If, for a fair comparison, it is assumed that only one travel lane is closed at a time, then the roadway could have a capacity of approximately 1,500 vehicles per hour for one direction. Looking at the hourly traffic counts for July, 2016 and 2017 for the segment of roadway, this is only exceeded between 7-9 pm and 6-7 am on average at the traffic counter just north of I-16, but is never exceeded at the tracker just south of the Savannah River (17). More congestion could be expected when working close to I-16, but congestion would be minimal further north on the project. The maximum exceedance for the southern part of the project was 500 vehicles in an hour. However, without a method of simulating the congestion, it is difficult to determine the exact impacts. Additionally, as can be seen in the difference in traffic flow and potential for congestion, this can vary widely from project to project. Therefore, it is worth mentioning that micro-milling is expected to progress twice as quickly as conventional

milling in terms of miles completed per night, but in the interest of developing a cost assessment that better represents the differences between micro- and conventional milling in general, this cost is left out. It is assumed that all the construction processes other than the milling machine are essentially the same, as supported by the contractor's comments. Traffic control information about what types of traffic control were used was not included because it was not available. The costs for the materials, construction, and the net present value (NPV) and equivalent uniform annual cost (EUAC) are shown in Table 3-1.

Table 3-1 – Costs associated with micro-milling and conventional milling

Cost	Micro-Milling	Conventional Milling
OGFC	$43,291	$43,291
SMA	$0	$59,178
Milling	$11,546	$13,939
NPV	$54,836	$116,408
EUAC	$5,843	$12,403

As can be seen in Table 3-1, micro-milling has substantial cost savings over conventional milling. This is primarily attributed to the reduction in asphaltic material being used, with $59,178 saved in SMA costs. Additionally, on this project, the micro-milling costs ($1.64/SY) were less than conventional milling (1.98/SY). The end result is a 53% savings when using micro-milling. This is much greater than the value found in the

first study because micro-milling costs were over 3 times as much as conventional milling in that study (15). Additionally, in the first study, micro-milling was assessed at a 10-year service interval and conventional milling at a 12-year service interval. Because of this great discrepancy in final values, both milling costs and service interval will be tested for sensitivity in the next section.

3.2.2   Sensitivity Study

Looking at the milling costs first, the micro-milling costs were increased to three times that of conventional milling, which were similar to the costs from 2007 for the first project (15). With this change, micro-milling saves 27% over conventional milling. The results are shown in Table 3-2. The analysis is clearly sensitive to changes in prices, so the next step is to determine how much more micro-milling needs to cost compared to conventional milling to make it cost the same. Achieving cost equivalence occurs when micro-milling costs 5.25 times more than the conventional milling. For the first project, micro-milling cost approximately 3 times as much as the average of conventional milling, weighted by area milled in Georgia for the year. It is unlikely that micro-milling will ever cost 5.25 times that of conventional milling now that contractors have more experience with it.

Table 3-2 – Costs when changing micro-milling to cost 3 times conventional milling

Cost	Micro-Milling	Conventional Milling
OGFC	$43,291	$43,291
SMA	$0	$59,178
Milling	$41,818	$13,939
NPV	$85,108	$116,408
EUAC	$9,068	$12,403

Next, it is of interest how the service interval impacts the comparison. The first assessment was to reduce the service interval of micro-milling to 10 years, the low end of the expected service interval. This only impacts the EUAC and results in a 45% savings by using micro-milling. The results are shown in Table 3-3. As was done for the milling cost comparison, the micro-milling service interval that makes micro-milling a less fiscally attractive alternative compared to conventional milling was found. With the contractor's costs for micro-milling and conventional milling and a 12-year service interval for conventional milling, the micro-milling needs a service interval of 5 years to be cost-effective. As was shown in Chapter 2, it is reasonable to expect micro-milling to last longer than 5 years, except when using for rut abatement on poor condition roads.

Table 3-3 – Costs when the service interval for micro-milling is adjusted to 10 years

Cost	Micro-Milling	Conventional Milling
OGFC	$43,291	$43,291
SMA	$0	$59,178
Milling	$11,546	$13,939
NPV	$54,836	$116,408
EUAC	$6,761	$12,403

However, in this scenario, micro-milling is less expensive than conventional milling. To address this, the analysis was repeated, using the cost of micro-milling as three times more expensive than conventional milling, as it was in 2007 for the first micro-milling project. In this scenario, the results showed that micro-milling must last for at least 8 years to be financially viable. This would still be a short life span for micro-milling based on the performance analysis in Chapter 2.

3.3 Summary

Based on the results, it can be concluded that the costs of micro-milling and thin overlay can vary from project to project, but the cost of micro-milling must be very high or the service interval be lower than expected to not be economically preferable to conventional

milling. Using milling costs for the recent I-95 project, micro-milling could save 53% the cost of conventional milling and resulted in a savings of $6,560 per lane-mile per year over the pavement's lifetime. If used on all the asphalt pavement interstates in Georgia, it could save over $500 million per year. In most situations, micro-milling is cost-effective and financially preferable to conventional milling.

CHAPTER 4.   ENVIRONMENTAL AND SOCIAL

SUSTAINABILITY

This thesis has shown that micro-milling and thin overlay is cost-effective and delivers acceptable performance that is comparable to conventional milling. The next step in assessing the sustainability of micro-milling and thin overlay is to quantify its environmental impacts. The objective of this chapter is to assess the environmental and social sustainability using data from a project in which the inside lane will be micro-milled and the outside lane has been conventionally milled; this will provide a good comparison of the two methods on the same roadway by the same contractor.

For this analysis, life cycle assessment (LCA) will be used. LCA is a tool that analyzes the environmental impacts of a process, system, or an entire industry from the beginning of the process (i.e. raw materials) to the end of life (i.e. landfill/recycling). This is called cradle-to-grave assessment. In LCA, this is accomplished through four steps: goal definition and scoping, inventory analysis, impact assessment, and interpretation (*29*, *30*). The first step sets the boundaries of the system being analyzed, which is based on the stated goal of the assessment. The inventory analysis catalogues all the inputs and outputs, including materials, energy, and emissions. The outputs from this step are used in the impact assessment to analyze the impacts on the environment and population. The interpretation step considers the whole analysis and provides recommendations. This analysis will walk through each step, but it will not get to the level of detail of direct impacts on human health, such as increased incidences of asthma. Any reduction in pollutants or energy use in comparison to conventional milling is considered a positive

impact. The following sections will discuss in detail each step; an analysis of the social sustainability is included at the end to complete the sustainability assessment.

4.1   Goal Definition and Scoping

The goal of this LCA is to compare and contrast the environmental impacts of two similar pavement preservation treatments: micro-milling and thin overlay and conventional milling and overlay. There are four general life stages of pavements: material acquisition, construction, use and maintenance, and end of life. This study will consider 3 of the 4 life stages: material acquisition, construction, and end of life. The use phase is not considered because the pavement/tire interaction is not well known, nor are the differences in surface characteristics between a thin overlay and the conventional overlay. Because the surface layer is the same in both options, it is assumed that their use phases are approximately equal in terms of environmental impacts. Maintenance is also not considered, as these are pavement preservation treatments themselves, and little to no maintenance is expected during the pavement's life. This study will also not go further than to quantify the emissions and material/energy use in the two options, as that should be sufficient to determine which is environmentally preferable. The unit of analysis will be a 12-foot wide lane for one lane-mile.

The analysis is performed very generally, but the construction process will consider a specific project on I-95. This project has both micro-milling and conventional milling, and the contractor was contacted for information to aid in the environmental analysis. At the time of writing, the conventional milling had been completed and the micro-milling

46

had not (scheduled for 2018), so the micro-milling values are based on the contractor's best estimation from past experience.

4.2   Inventory Analysis

Both conventional milling and micro-milling can be divided into 4 sub-systems: raw material acquisition and production, construction, use, and end of life. Each sub-system will be described in more detail in this section, including their components, inputs, and outputs. An overview is provided in Figure 4-1. Although transportation is not included as a component or sub-system, it is an important piece of the life cycle of an asphalt pavement and is included in every sub-system and most components.
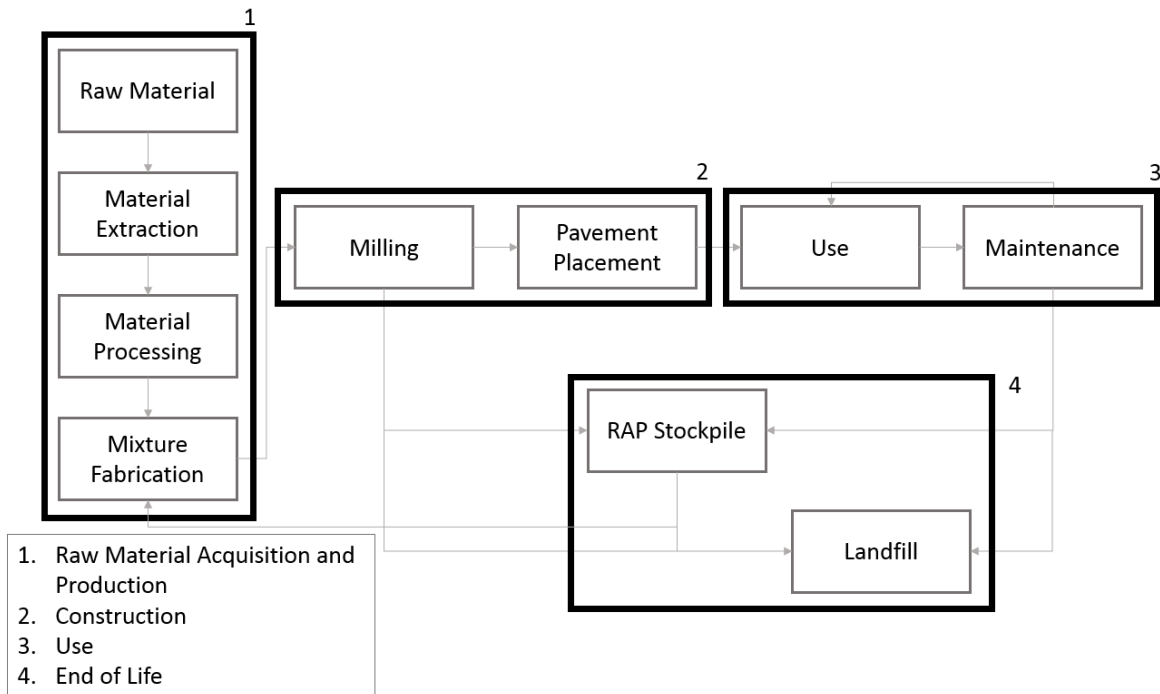
Figure 4-1— Sub-systems and components of the milling and overlay process

4.2.1   Raw Material Acquisition and Production

This sub-system consists of 4 components: raw material, material extraction, material processing, and asphalt mixture fabrication. The starting inputs for the process are raw material and energy, which are added throughout the entire process, and the outputs are the asphalt mixture and emissions.

When making asphalt, the raw material is typically petroleum. First, crude oil must be extracted, which generally requires drilling, primary recovery during which natural methods cause the oil to come to the surface, and/or secondary recovery during which enhanced methods are needed, such as injecting fluid to increase pressure (*31*). Drilling and secondary recovery require energy inputs into the system.

Once extracted, the crude oil is transported to a petroleum refinery. Asphalt is one of the many products of refining petroleum. To begin the process, crude oil is transported to the refinery, which can be accomplished via pipe, tanker ship, rail, truck, or a combination of these (*32*). Each of these modes takes energy and generates emissions. Once delivered for refining, crude oil must have water, contaminants, and salts removed. Sometimes, this can be done through settling in tanks, but if the salt content remains too high, it must be desalted. Fresh water is added to separate the emulsion of water and salt from the oil, which is performed at approximately 200-300 degrees Fahrenheit (*32*). Therefore, this step requires the addition of both water, which could be treated onsite and reused, and energy to the system.

Once desalted, the oil can be moved to distillation towers. Asphalt undergoes two phases of distillation. First, the oil is heated to approximately 700 degrees (*32*) and sent to

atmospheric distillation towers (*33*). The atmospheric distillation separates the lighter hydrocarbons, and the residue is sent on to vacuum distillation towers (*33*). The residue from this process can be taken as asphalt, or it can be cracked and turned into another material or mixed and manipulated through additives to create a different type of asphalt (*32*). These processes also require large energy inputs. Finally, the asphalt is prepared for mixing with aggregate, typically as emulsified asphalt (*33*).

The asphalt only makes up a small percentage of the overall pavement. The majority is aggregate. Natural aggregate is typically produced in a quarry or mine where in situ rock is turned into aggregate. This involves blasting or digging rock from the quarry walls; then, screens and crushers are used to reduce the aggregate to the desired size. (*34*) This, too, requires energy input and results in dust emissions. As with oil used for the asphalt, rocks are a limited resource and materials use must be considered in environmental impacts as well.

The last step in producing the paving material is to mix the asphalt with the aggregate. This can be done on or off site using either a drum-mix facility or a batch mix facility. The mixture must be heated during this process to make it workable. The mixture is then transported to either the job site or storage. (*33*)

Overall, it has been shown that the petroleum refining necessary to fabricate asphalt involves very high heats, up to 700 degrees Fahrenheit if no cracking occurs, throughout the process and requires large amounts of energy. The refining of petroleum is also known for its emissions. Laws have put in place strict codes limiting emissions and water use from both refinery plants and asphalt processing plants (*33*). Reclaimed asphalt pavement (RAP)

can also cut out much of this process, just needing to be re-mixed, sometimes with additives to improve the quality of the asphalt, and re-laid. This still has the energy and emissions associated with the last component of the sub-system but can greatly reduce emissions, material use, and energy use by not returning to the raw materials step.

4.2.2 *Construction*

Much of the construction process was detailed in Chapter 1. There are two major components to the construction process: milling and pavement placement. The inputs into this sub-system are the asphaltic concrete from the raw material acquisition and production stage and energy. Outputs include a completed pavement, but also emissions, including emissions from the construction equipment and dust from the process. Emissions can also be generated by congestion from the traffic control operations if congestion occurs.

Much of the construction process is the same for micro-milling and conventional milling. The primary differences are in the number of paving passes needed and that micro-milled surfaces can be opened to traffic, allowing more construction flexibility. To keep traffic flow, conventional milling requires that the milling and the first overlay (leaving only the OGFC off) must be done in the same construction period. However, the micro-milling process can be more intensive and slower due to the higher number of teeth on the drum, potentially resulting in different amounts of fuel usage per mile milled. This was not tracked by the contractor, so the exact change is not known. Typically for this contractor, and as a representative example, micro-milling progresses at 15-20 ft/min, and conventional milling at 30-35 ft/min (*35*). Micro-milling also requires extra or slower sweeping with a broom truck to remove all the dust from the surface.

The construction timing also impacts both emissions from automobiles and construction equipment. Congestion caused by construction is heavily dependent on when construction is performed. If construction is performed at night, allowing traffic to flow during the day when vehicle flow is higher, then the increased emissions from traffic could be low to none. In the case of interstate construction work, the work is typically done at night as was done on the analyzed project (*35*). Construction timing is more flexible using micro-milling, which only needs a lane to be closed during the milling and the overlay processes; between milling and overlay, traffic can flow on the milled surface. The number of construction periods needed can impact both the congestion caused by the construction and the emissions from the equipment. Conventional milling and overlay takes longer because milling and overlay can only progress as far as can be fully completed in one construction period. Micro-milling and thin overlay, in contrast, can spend an entire construction period milling and another one overlaying. Although the micro-milling machine must progress at a speed approximately half that of conventional milling, the micro-milling project is anticipated to progress an average of 3 miles per night, whereas conventional milling progressed at an average of 1 mile per night (*35*).

Once construction is complete, no work is needed on the road until the end of its service interval. It has entered the use phase. Emissions during the use phase are generally considered to be the highest of all the stages because it includes emissions from the vehicles using the road, but without knowing details about the pavement texture and pavement/tire interaction it is not possible to determine a difference in use phase emissions between the two methods. Therefore, next the end of life sub-system will be discussed.

4.2.3   End of Life

When the pavement is removed at the end of life, it can go to two destinations: RAP stockpiles or landfills. RAP stockpiles is the environmentally preferable use of removed asphalt. In Georgia, the maximum amount of RAP allowed for use on a project is 30%, but the amount allowed is dependent on tests of the RAP stockpile and the required gradations (*36*, *37*). Therefore, the outputs of this system could include either waste material and/or RAP that is fed into Sub-system 1 (see Figure 4-1). This phase also requires energy input and produces emissions during the transportation of the material to the stockpile or landfill.

4.3   Impact Assessment

With the inputs and outputs of all the sub-systems and components considered, an impact assessment can be performed. The Pavement Lifecycle Assessment Tool for Environmental and Economic Effects (PaLATE) is the chosen tool for this analysis (*38*). PaLATE is a life cycle assessment tool designed for pavement construction LCA and utilizes a large database of publicly available data from sources such as the Environmental Protection Agency. It is an integrated, hybrid, and streamlined LCA tool. It is integrated because it combines environmental and economic assessments, but only the environmental part was used here. The combination of a process-based and matrix-based (economic input-output matrix (EIO-LCA)) life cycle assessment method for calculations makes it a hybrid LCA. The tool is considered streamlined because it is simplified for what is needed for pavement construction LCA in Microsoft® Excel spreadsheets (*38*).

There are three types of data used in the tool. They are emissions, construction process, and human toxicity potential (HTP) (*39*). Nathman et al. discovered that,

unfortunately, the HTP module still needs improved data for accurate results, so it will not

be used in this analysis (*39*). Nathman et al. also determined some of the limitations of the

software, which include the assumption that all on-site processes are identical and the

reliance on EIO-LCA, which has its own assumptions and limitation (*39*). Despite these

limitations, the tool is still effective for agencies wanting to perform LCA analyses of their

pavement construction and maintenance practices. Many studies have been performed

using the tool, including a study on parking infrastructure (*40*), pavement preservation (*41*),

cold in-place recycling (*42*), and in situ pavement recycling (*43*), which demonstrates its

usefulness to agencies. It was decided that this is the most effective tool for this analysis.

As a spreadsheet based tool, there are a variety of inputs needed in the model. The

data for these inputs come from the contractor for the 13-mile-long project on I-95 in

Georgia. The project was originally let as a micro-milling project but was changed to

conventional milling on the two outside lanes and micro-milling on the inside lane. This

provides the opportunity to compare micro-milling and conventional milling on the same

project with the same contractor. Some data was not available because it was considered

confidential or the contractor did not collect it. When data was missing, default data from

the program or the best approximation was used. For example, all the operating data for

the machines used for the milling process was not available, so the closest machine already

included in PaLATE was used. Additionally, it was not possible to get the mix design for

the paving material, so GDOT's standard mix designs (*44*) were used. These changes will

not have a major impact on the results, as will be shown.

The analysis is performed on a 12-ft-wide lane for 1 mile. Micro-milling and

conventional milling have a 7/8" layer of OGFC based on GDOT specifications.

Conventional milling has an additional 1.5" layer of SMA according to GDOT specifications. RAP was used in the SMA, but the percentage is unknown. A RAP percentage of 5% was assumed, but a sensitivity study will be conducted to test sensitivity to this parameter. Transport distances averaged 6 miles, according to the contractor on the project. The asphalt plant uses an Astec Double Barrel, which is a type of drum-mix machine. It has reduced emissions compared to traditional drum-mix plants (*45*), so the fabric filter-controlled drum-mix in PaLATE was used to approximate this.

The outputs include the energy usage, water usage, global warming potential, and air pollutants. The majority of the total in each category was caused during the material production phase. For example, during the material production phase for micro-milling, 98.2% of the total energy used in the entire process is used. For conventional milling the number is similar at 98.6% of the total energy is used during the material production. This discrepancy is shown in Figure 4-2. Even with only a 6-mile travel distance, the equipment and processes (during the construction phase) contribute only approximately ¼ of the energy use of the materials transportation, and a meager 0.4% to the total. It is clear that efforts to reduce the environmental impacts of milling operations should focus on reducing the amount of asphalt material needed, which micro-milling effectively does. Figure 4-3 and Figure 4-4 show the water usage and global warming potential, respectively, to demonstrate that materials production dominates the environmental impact in each category. Furthermore, micro-milling reduces impacts in each category assessed using PaLATE by just over 60%, as shown in Table 4-1. Micro-milling reduces material needs by 63% in this scenario, which is similar to the overall reductions in environmental impacts, and further demonstrates the benefits of reducing material use.
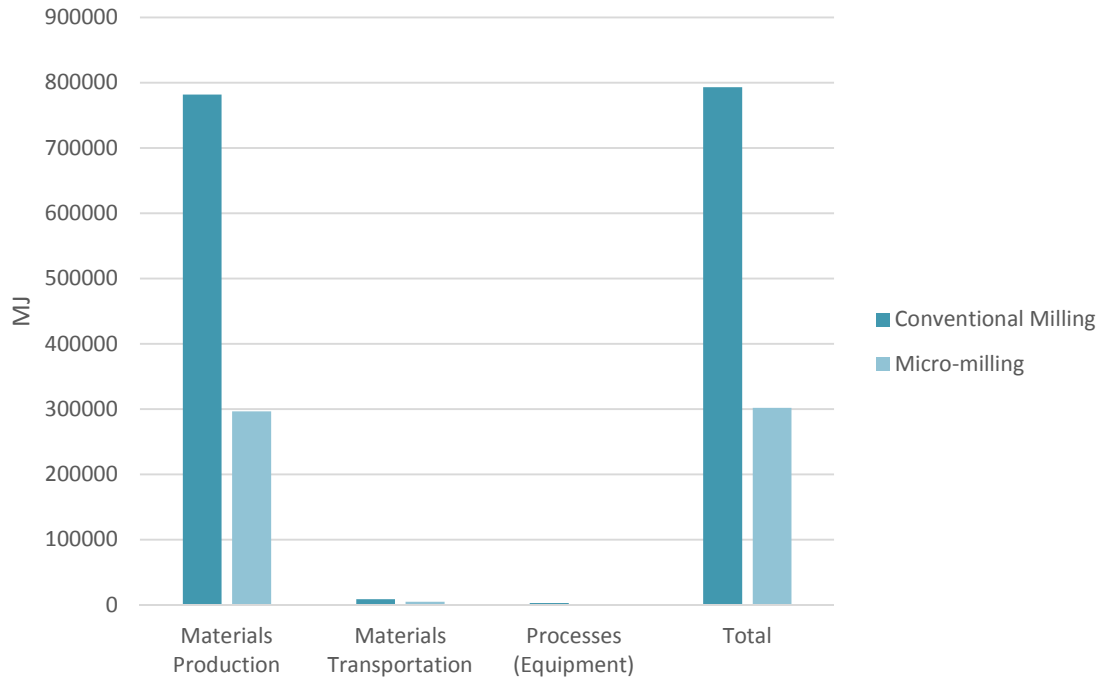
Figure 4-2 – Energy usage in Mega Joules (MJ) for each process of conventional and micro-milling
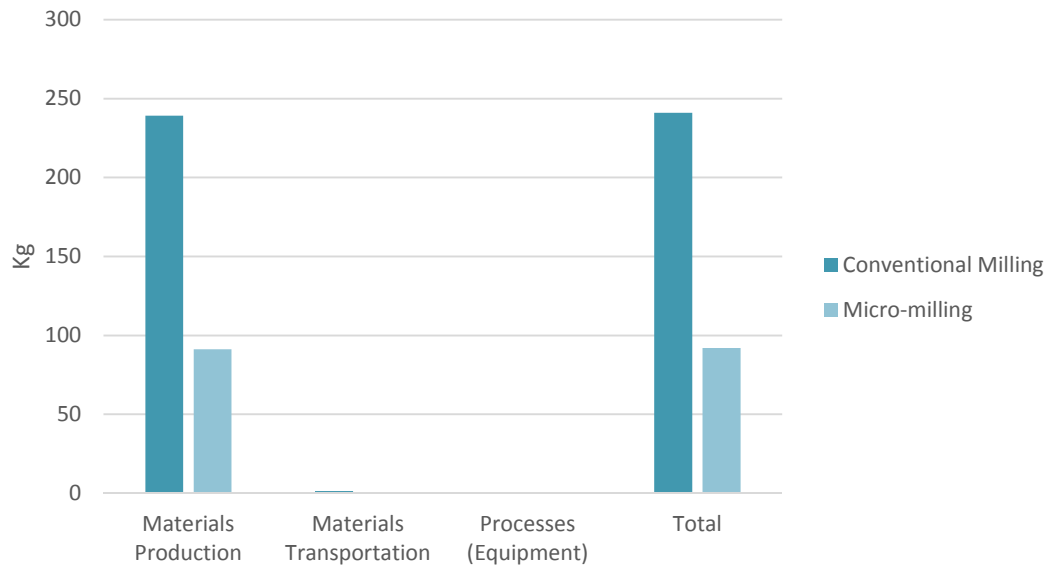
Figure 4-3 – Water usage in Kg for each process of conventional and micro-milling
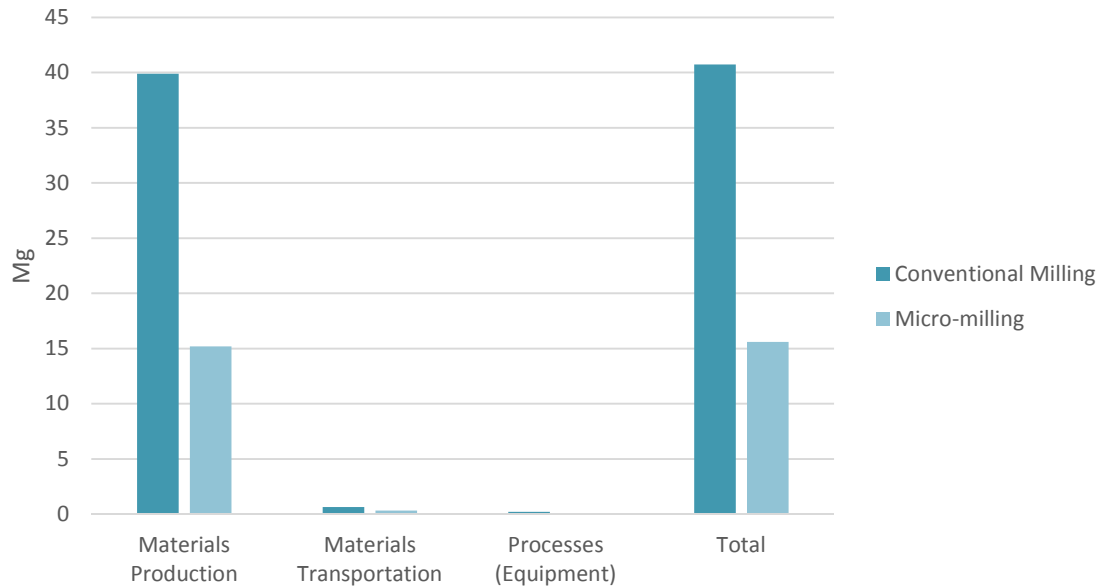
Figure 4-4 – Global warming potential in Mega-grams (Mg) for each process of conventional and micro-milling

Table 4-1 – Total impacts for conventional and micro-milling and % reduction when choosing micro-milling instead of conventional milling

Impact	Conventional Milling	Micro-Milling	% Reduction Using Micro-Milling
Energy [MJ]	793,070	301,978	61.9%
Water Consumption [kg]	241	92	61.8%
CO_2 [Mg] = GWP	41	16	61.7%
NOx [kg]	259	103	60.2%
PM10 [kg]	182	71	61.1%
SO_2 [kg]	8,714	3,215	63.1%
CO [kg]	143	55	61.6%

4.3.1   Limitations

This model, although useful, cannot perfectly model the differences between these two construction practices, nor does it break down the impacts to each component of the sub-system (i.e., there is no information available to determine which part of the materials acquisition and production phase results in the most emissions). Overall, the construction practices are very similar for both micro-milling and conventional milling, except that a micro-milled surface can be opened to traffic. This allows the contractor to mill during the entire construction period (all night in this situation), whereas the conventional milling operation must be stopped early to allow for paving. Therefore, although micro-milling requires a slower milling speed (15-20 ft/min) than conventional milling (30-35 ft/min), the daily production rate for micro-milling is 3 times that of conventional milling (*35*). The stopping and starting with conventional milling can result in more cold starts and more emissions than using one set of machines per night. It was not possible to effectively model this in the PaLATE program. This is likely not a significant impact, as the construction processes only contributed approximately 0.4% of the environmental impacts, but it is worth noting. The machines were, also, not the same as those used in this project, but, as the main goal of this thesis is to form a general comparison, this situation should not impact the overall comparison. However, to address some of these limitations and support the claim that this situation does not have a substantial impact on the results, a sensitivity analysis will be performed here.

4.3.2 Sensitivity Analysis

The first sensitivity analysis will consider the transportation distance. The effect of transportation distance on the overall emissions is impacted by the actual travel distance. However, the transportation distance would be unlikely to be far enough for the environmental impacts to match the impacts from material production, which is the main contributor to environmental impacts. For this micro-milling project, a travel distance of 395 miles was needed for transportation impacts to be approximately equal to the environmental impacts from material acquisition and processing. Three hundred ninety-five miles is nearly 1/5 of the distance from Georgia to California. This travel distance is unlikely to happen and would be even more unlikely with conventional milling, which would require travel distances of 540 miles to have transportation exceed production. Adding 10 miles to the travel distance may be a more useful calculation. Table 4-2 shows the increase and percentage impact on the total for each assessed category. As can be seen, it has the greatest impact on the air emissions, especially NOx and particulate matter, which are of high concern in diesel vehicles, such as large trucks that would transport paving materials. This is an important consideration, and efforts to reduce transport distances are encouraged, but it has a minor impact on this thesis' comparison because transport is not inherent to the milling processes and depends more on the location of the stockpiles and mix sites. However, it still has some impact, as more transportation is needed to move the larger amounts of material used in conventional milling. Overall, the impact is minor and had only a small effect on the values for % reduction using micro-milling in Table 4-1 and as shown in Table 4-3.

Table 4-2 – Sensitivity results for increasing travel distance by 10 miles

Impact	Conventional Milling		Micro-Milling	
	Change	% Change	Change	% Change
Energy [MJ]	14314.49	1.77%	7491.88	2.42%
Water Consumption [kg]	2.44	1.00%	1.28	1.37%
CO2 [Mg] = GWP	1.07	2.56%	0.56	3.47%
NOx [kg]	57.01	18.06%	29.84	22.48%
PM10 [kg]	10.95	5.69%	5.76	7.52%
SO2 [kg]	3.42	0.04%	1.79	0.06%
CO [kg]	4.75	3.22%	2.49	4.35%

Table 4-3 – Change in comparison values from increasing transportation distance 10 miles

Impact	Conventional Milling	Micro-Milling	% Reduction Using Micro-Milling	Original % Reduction
Energy [MJ]	807384.8	309,470	61.7%	61.9%
Water Consumption [kg]	243.4336	93	61.7%	61.8%
CO2 [Mg] = GWP	41.80818	16	61.3%	61.7%
NOx [kg]	315.7474	133	58.0%	60.2%
PM10 [kg]	192.5642	76	60.3%	61.1%
SO2 [kg]	8717.86	3,217	63.1%	63.1%
CO [kg]	147.3831	57	61.2%	61.6%

The RAP percentage can also vary across projects. To consider the sensitivity of this, 30% RAP was used for the SMA and none for the OGFCs by over 50% in each category compared to conventional milling.

Table 4-4 shows the change in outputs for conventional milling, as this did not impact the micro-milling, which uses no SMA. This had a greater impact on the overall end results than the transportation distance, as shown in

Table 4-5. This makes sense, as reducing material usage was found to be the best way to reduce environmental impacts. However, at the highest percentage of RAP allowed in Georgia, micro-milling still reduces environmental impacts by over 50% in each category compared to conventional milling.

Table 4-4 – Sensitivity results for conventional milling when including 30% RAP

	Conventional Milling	
Impact	Change	% Change
Energy [MJ]	-113,927.17	-16.78%
Water Consumption [kg]	-41.56	-20.84%
CO2 [Mg] = GWP	-6.65	-19.50%
NOx [kg]	-31.15	-13.69%
PM10 [kg]	-28.42	-18.55%
SO2 [kg]	-27.66	-0.32%
CO [kg]	-23.76	-19.99%

Table 4-5 – Change in comparison values when using 30% RAP

Impact	Conventional Milling	Micro-Milling	% Reduction Using Micro-Milling	Original Reduction
Energy [MJ]	679143.2	301977.7	55.5%	61.9%
Water Consumption [kg]	199.4322	92.072	53.8%	61.8%
CO2 [Mg] = GWP	34.09047	15.60117	54.2%	61.7%
NOx [kg]	227.5843	102.8872	54.8%	60.2%
PM10 [kg]	153.1955	70.73647	53.8%	61.1%
SO2 [kg]	8686.777	3214.99	63.0%	63.1%
CO [kg]	118.8684	54.73683	54.0%	61.6%

When considering the sensitivity of the program to the equipment used, it was determined that the impacts are so minor that it could not be effectively shown using tables. Changing the paver resulted in a maximum overall energy usage change of 11 MJ for micro-milling, a change of 0.003%. The changes in the other categories did not appear in the results, as they were so small. This supports the claim that not having exact machines in the analysis has a negligible impact on the overall analysis.

4.4 Interpretation

There are three major conclusions based on the results of the impact assessment. The first conclusion is that micro-milling and thin overlay is a more environmentally friendly

construction practice than conventional milling, reducing environmental impacts by approximately 62% for energy use, water use, and global warming potential. Therefore, it is recommended that micro-milling and thin overlay be used whenever it is an option. The second conclusion is that the highest environmental impacts in all three categories comes from the materials acquisition and production. Efforts to reduce environmental impacts in the roadway construction industry should focus on this part of the process. One well-known method that significantly reduces the impacts from this sub-section is asphalt recycling. It is recommended that up to 30% of RAP, as recommended by GDOT and Norouzi et al., be used as much as possible (*36*, *37*). Finally, emissions are sensitive to the travel distance of materials transported to/from construction sites and RAP usage, but do not have a substantial impact on the results of the micro-milling or conventional milling comparison. However, using local materials and RAP as much as possible is highly recommended.

Although these recommendations have been generally known in the industry, it is beneficial to quantify these impacts for a better understanding of how construction impacts the environment and more specifically, to gain a stronger understanding of micro-milling and thin overlay for pavement preservation.

4.5 Social Sustainability

A sustainability analysis would not be complete without an analysis of the social sustainability of the system. This is rarely considered in pavement preservation, likely because it has little to no impact on equity. Construction can have impacts, however, on safety, traffic, and noise. An understanding of the social impacts of pavement construction,

even a qualitative one, can benefit public relations and perceptions of the projects, which can, in turn, save money and reduce environmental impacts.

4.5.1 Safety

Micro-milling has two safety benefits over conventional milling. For drivers, the small drop-off that allows the roadway to be open to traffic prior to the overlay increases safety. It is only possible that this be opened to traffic because the drop-off between lanes is too small to cause concern that a driver will lose control when traversing it. The second safety benefit is for the construction workers. Because micro-milling can be performed more quickly, they are exposed to interstate traffic for a shorter period of time, reducing risk of being hit by a passing vehicle.

4.5.2 Traffic

Because the micro-milled surface can be opened to traffic, construction staging is more flexible, and the overall construction can be performed more quickly. Because night-time construction has little impact on traffic (and this project only had nighttime construction), and overall construction time is reduced, reduced traffic congestion is expected. This has not been quantified in this analysis for the reasons mentioned in Chapter 3, but future research could quantify this benefit.

4.5.3 Noise

Construction is always noisy and can have impacts on people or animals in the surrounding area. The noise difference between micro-milling and conventional milling

was not discernible to the contractor and is considered negligible. However, micro-milling has the benefit of having a potentially shorter construction time, which reduces the total amount of time noise pollution from the construction occurs.

4.6 Summary

Overall, it was found that micro-milling produces 61.7% percent fewer greenhouse gases, uses 61.8% percent less water, and uses 61.9% percent less energy than conventional milling operations. The drive-able surface and flexible construction schedule allow for improvements in safety, traffic flow, and noise reduction. Micro-milling and thin overlay is both environmentally and socially more sustainable than conventional milling. It is also more cost-effective, although it is important to remember that it can only be used under certain circumstances. When a road qualifies for micro-milling, it is strongly recommended that the option be used.

This treatment is favorable for transportation agencies and the public because of its performance and its economic, environmental, and social benefits. However, it may not be favorable to construction contractors because the reduction in paving material use reduces profits. There is potential to offset this by optimizing how contractors use their personnel and equipment, as micro-milling only needs the milling equipment during the milling night and the paving during the paving nights, so the unused teams can work on another project at the same time. Training is needed to promote the application of this new treatment nationally and globally. In addition, further performance analysis beyond Chapter 2 of this thesis is needed to better understand which pre-existing conditions qualify a road for micro-milling and thin overlay. There is still room to improve the treatment and optimize

performance. The next chapter will refine the 3D collection of the quality control measure

and provide initial findings regarding the validation of the measure.

CHAPTER 5. RIDGE-TO-VALLEY DEPTH AUTOMATIC COMPUTATION USING 3D SENSING AND INITIAL FINDINGS

Ridge-to-valley depth (RVD), described in Chapter 1, is a quality control measure used by GDOT for its micro-milling and thin overlay operations. It measures the difference between a pavement surface's highest peak and lowest valley over 100 mm, as shown in Figure 1-2. This value was designed to evaluate the ability for water to run off the surface without being trapped. Tsai et al. (*19*) have shown that RVD can be measured using 3D sensing technology, but the process still needed to be automated to be useful. Additionally, as mentioned in Chapter 1, the cutoff point of 3.2 mm was originally set by statistics and engineering knowledge and was not based on pavement performance data. With the 3D sensing images collected in 2011 from the first micro-milling project on I-95 and the performance data collected from 2012-2017, it is possible to begin assessing whether this value is reasonable. Due to the high resolution of 3D sensing in comparison to the point lasers used for gathering RVD previously, some computation adjustments needed to be made, which will also be detailed in this chapter.

This chapter will accomplish two goals. The first is to detail how the RVD computation was automated and adjusted. The second is to describe the general findings from the I-95 data to determine whether a mean value of 3.2 mm is a reasonable micro-milling construction quality control value.

5.1 Automation

The automation of the RVD measurement was carried about by many people as the Matlab® code was passed on. The original code was written many years prior by Dr. Feng Li, but the next author determined that the code was not sufficiently robust and was written in a manner that made it excessively difficult to edit. Therefore, a new RVD code was rewritten from scratch. Ms. Segolene Brivet was the primary author of the newly-written code, which calculated both faulting and texture values, named the Faulting Evaluation and Texture Analysis (FETA) code. When Ms. Brivet passed on the code, it did not automatically calculate RVD for multiple images by clicking one button, so a batch processing capability was added. In attempts to match the computation to ground truth, the outlier removal and filter portions of the code were adjusted. The output formats were also changed to be more useful, and a code was written to process the outputs to give aggregated RVD values and histograms as needed. In this chapter, the overall code will be described, but it will focus on the parts added or manipulated to improve the code after Ms Brivet passed it on. Figure 5-1 is a flow chart of the code; the parts will be described in this chapter.
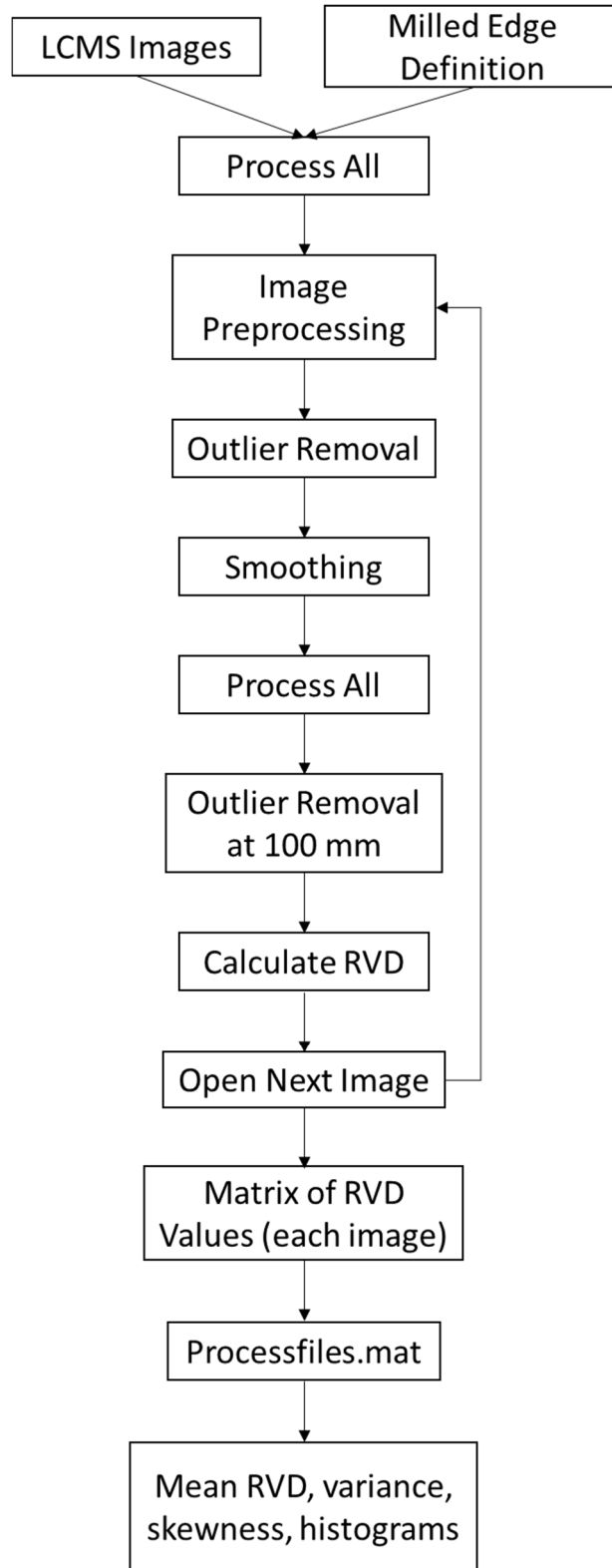
**Figure 5-1 – Flowchart of the code**

Automation is necessary because the quality must be checked quickly to reduce the amount of construction that must be re-done if the measures are not met. The data used to test this varied, but the final data sets were from an approximately one-mile section on the first I-95 micro-milling project, the same section used in Chapter 2, and asphalt boards that were produced in-house and scanned using a highly accurate 3D scanner as ground truth.

5.1.1   Interface

Before discussing the details of the code, an initial description of the user interface and inputs and outputs is needed. A screenshot of the user interface is shown in Figure 5-2. There are two major components to the code: a portion that calculates faulting and another than analyzes texture. The faulting components are to the right of the LCMS images and are not used in this analysis. In the upper left, buttons to open the two types of data (LCMS and LS40) this code accepts are given. LCMS data was used for this analysis. For visualization purposes, the left and right intensity images are shown. The yellow lines on the images show the boundaries for analysis from an input comma-separated value (CSV) file. Underneath the images, the image of interest can be selected or a profile can be viewed. In the results box under this is where the texture measurement information exists. When a CSV file is included, the user can choose whether to calculate over the whole image or the area. The "Run" button will calculate for just 1 image, whereas "Process All" is available if a CSV file is added. "Process All" will start the batch processing algorithm. To input a CSV file, the "Select File" button needs to be selected. There are also a variety of options for the RVD computation shown here. These include the baseline and where to calculate within the area (drop down menus), whether to use outlier removal and the number of

standard deviations to consider as an outlier, the filter type, and the baseline orientation. The results for MPD, RVD, and MTD are also shown. The histogram shows the histogram of MPD results. The outputs include these results and saved MAT files of RVD for each image.
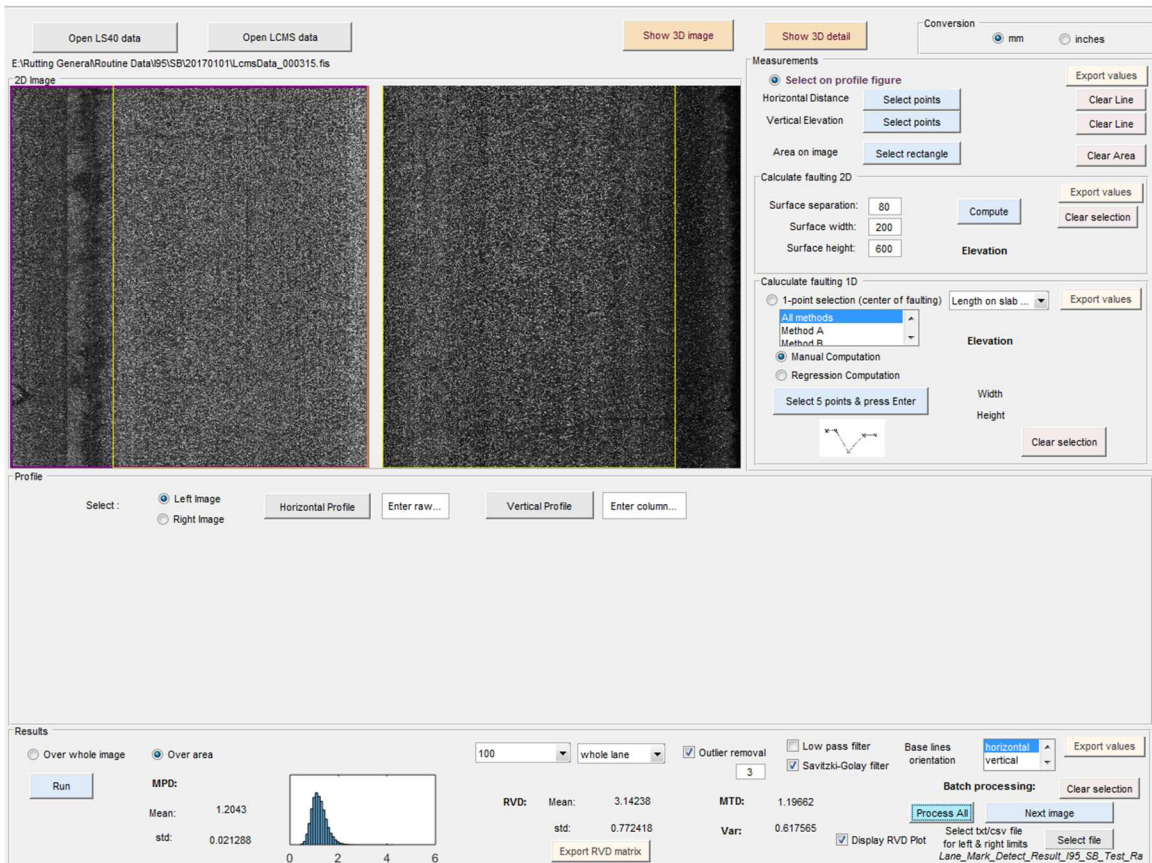
Figure 5-2 – User interface for the FETA code

5.1.2   Pre-Processing

Some minor pre-processing is needed to run the batch processing part of the FETA code. The main pre-processing step is to define the milling area, which is approximately defining where the lane markings would be if they had not been milled off. To do this, the user must input a CSV file that defines the left and right edges of computation. This can be

created using an in-house, lane-marking detection code, but no markings will be detected, as none exist. However, the code does have an interface for visually selecting the location. Another option is to create a CSV file and assume a left and right edge of the milling area. The values range from 0-5160 pixels. Next, the user must test the assumed values on a few images to see the accuracy, which can easily be seen when choosing to display the RVD values; then, the user can adjust accordingly. It is important to note that the chosen edges are also from where the wheelpath locations are calculated.

The code does not do analysis for a small area or region of interest, but this can easily be done if one knows the region using the output RVD file. The output RVD file is a matrix, so the region of interest can be extracted from the output RVD by indexing.

5.1.3 *Calculating RVD for a Single Image*

The user interface for FETA gives a variety of options. Most buttons for processing a single image were set up by Ms. Brivet. These options include selecting which image to calculate over (right or left), the baseline to be used for the measurement (typically set to 100 mm), a toggle for the outlier removal, and toggles for the different filter options. These were discussed above for Figure 5-2.

5.1.3.1 Outlier Removal

When calculating over a single image, the first step is the pre-processing of the image. This was implemented by Ms. Segolene Brivet, but it is briefly described here for completeness. This includes rescaling the image so the minimum value of the image is zero and setting the missing values to NaN. Next, the outlier removal is performed. This process is first performed on each profile. Each profile is initially smoothed to remove the slope.

71

Then the standard deviation and median are calculated. When a missing value is found or a value that is more than 3 standard deviations from the median, the previous value in the profile (aka vector) is used replace the value. Three standard deviations are used when assuming a normal distribution, which was done here. This was also used in the initial code by Dr. Li. When the first value needs to be replaced, the first valid value of the profile is used. When an entire profile is missing, it is left as NaN.

5.1.3.2   Smoothing

After the outlier removal, a smoothing algorithm is applied. Three smoothing algorithms were considered: Butterworth, low-pass, and Savitzky-Golay filters. The Butterworth filter is the filter used by Proval for calculating the International Roughness Index (IRI). It was, not implemented because IRI is a very different measurement from RVD in the area used to calculate it and the type of signal. A low-pass filter was initially included in the code by Ms. Brivet. The low-pass filter ignores values below a certain cut-off frequency and attenuates those above it. Because the noise caused spikes, this seemed a reasonable filter choice. However, the Savitzky-Golay filter was considered more effective for this computation because it smooths the data with minimal distortion, resulting in smoothed data that is more like that of the true surface. The Savitzky-Golay filter was also originally included by Ms. Brivet and was recommended by her. However, the filter still needed the parameters refined. Both filter's parameters were refined to give the closest values to ground truth, then the choice of the Savitzky-Golay filter was confirmed. Examples of the same profile filtered by the Savitzky-Golay filter and low-pass filter are given in Figure 5-3. Note that the shape of the profile is not as well kept with the low-pass filter, especially at the peaks. Some notable locations are circled in Figure 5-3.
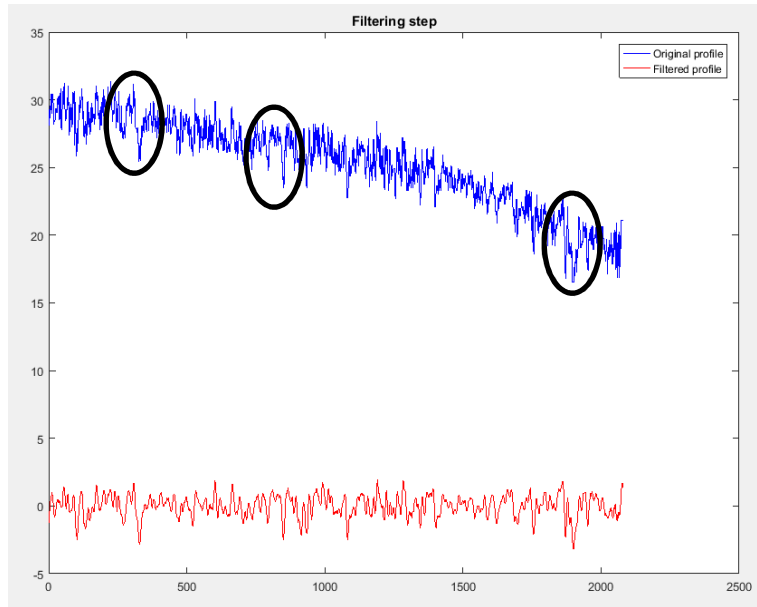
(a)
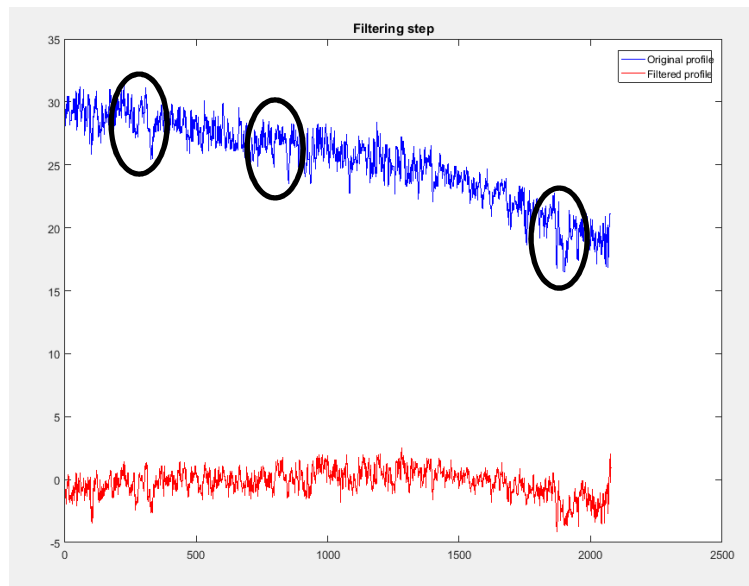
(b)

Figure 5-3 – A comparison of the Savitzky-Golay Filter (a) and the low-pass filter (b)

To smooth the data most correctly, a ground truth was needed. Asphalt boards made in-house for a previous project were used, as they had already been scanned and pre-processed to create the best representation of reality. These asphalt boards are

73

approximately 1' x 1' squares of asphalt pavement. These also had true ground truth tied to them as the boards were used to test a code to detect aggregate loss. So, there is ground truth in terms of calculated aggregate loss on the boards and an actual volume of aggregate removed. Five scans were taken, each with more aggregate removed, resulting in progressively higher RVD values over the board. Each board is 250 mm wide, so only two RVD readings were possible along the board. The boards were scanned using a FaroArm scanner. The scans were then pre-processed to fill in missing values using an outlier removal process similar to the one used in the RVD computations. The board is also corrected for any tilt in the surface by using least square minimization. The end result of the pre-processing was used for this study and is shown in Figure 5-4.
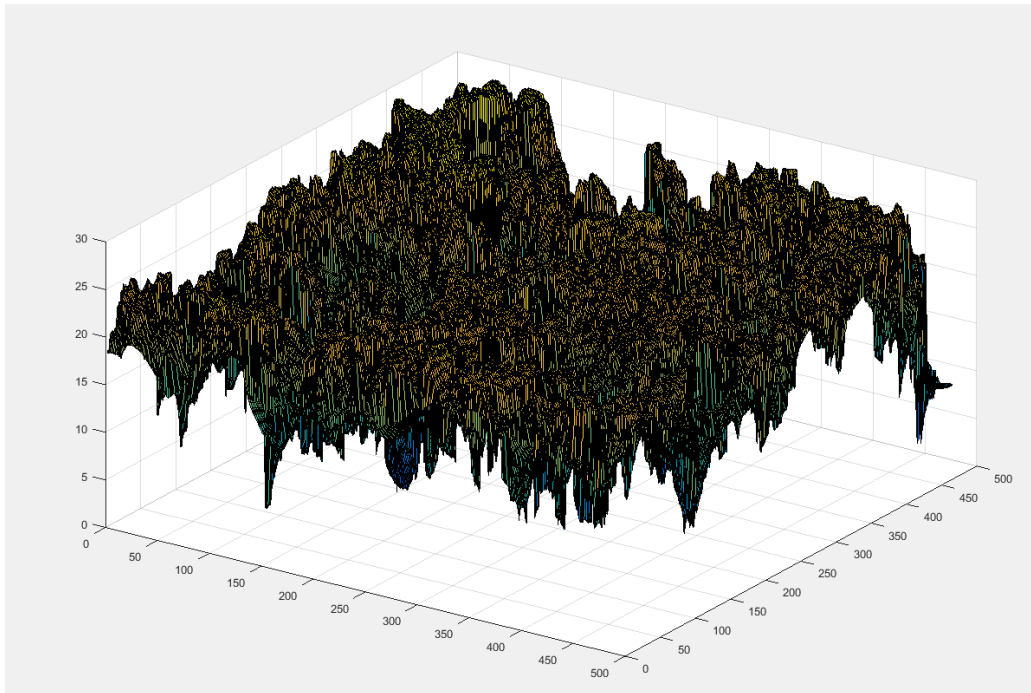
Figure 5-4 – End result of the pre-processing of the FaroArm data

In addition to the 3D scanner, the Georgia Tech Sensing Van was used to collect LCMS images of the boards. The FETA code was used to calculate RVD based on the

FaroArm scans without using any filtering. Then, the section of the LCMS images with the board was used to calculate the RVD. The filters were applied to the LCMS images and adjusted until the results most closely matched the five FaroArm scan RVD results, although a perfect match for all scans was not possible. For the chosen Savitzky-Golay filter, the results showed that the best parameters were third order with a frame length of 15. Some example outputs are shown in Figure 5-5.
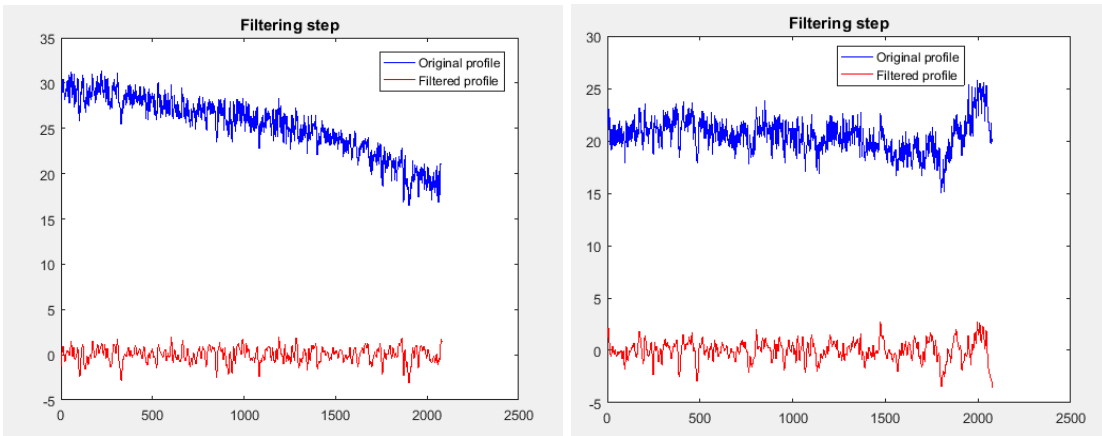
Figure 5-5 – Examples of profiles before (blue) and after (red) using the Savitzky-Golay Filter

5.1.3.3   RVD Computation

Once the profiles have been smoothed, the RVD computation can be performed. As mentioned, it is performed based on a specified baseline measurement; however, the baseline is always 100 mm. This value was chosen to align with the MPD computation specified in ASTM E1845 (*22*). GDOT uses a point laser to calculate RVD, but when calculating it using full lane width 3D sensing data, the transverse direction is used for two reasons. The first is that this better represents the direction of water flow, which is the original basis behind the development of the measurement. The second is that the 3D

75

sensing data has a better resolution in the transverse direction (1 mm) than in the longitudinal/driving direction (5 mm). When taking strictly the highest and lowest point over 100 mm, this computation can be very sensitive to noise or other unusual changes in the signal. It is more likely when having 100 points to calculate over than 20 points to calculate over that a higher or lower point will be found. Compounding this problem, the GDOT point laser calculated just in the wheelpath along a single line, but with the GTSV, analysis over the whole lane width is possible. For these reasons, some more measures were needed to ensure the computations on sections found to be less than 3.2 mm in the field; these gave values less than 3.2 mm with the 3D sensing data.

The first extra measure employed was to include a second outlier removal, this time on the 100-mm scale, to find any more local outliers. The next was to calculate a mean of an upper percentile of the highest and lowest points to adjust for the increased number of data points and the higher results in the transverse direction. The percentile was chosen by first interpolating the images so that the same number of points were in the transverse and longitudinal directions. Then, the RVD was calculated in both directions. The results of this analysis were consistent with the previous paper by Lai et al. (*18*) that observed a 22% difference in the transverse and longitudinal direction using the Circular Track Meter (CTM) test. This was put directly into the code by taking the mean of the upper 22% for the peaks and the lowest 22% for the values as the peak and valley for calculating RVD. The mean is taken rather than the strict percentile for two reasons. The first reason is that taking 22% from the high and low points removed 44% of the entire set. The second reason is that, taking just 11% from each resulted in just 1 or 2 peaks, so the mean of 22% can better represent the range of values in the 22 percentile. This was tested by calculating in

both the transverse and longitudinal directions, interpolating the points to have the same number as in the transverse direction. The transverse direction had the 22 percentile applied, but this was removed for calculating the longitudinal direction. The results came out with a difference of 1.6%. However, a 1.6% difference is negligible when discussing it at the mm scale. The entire final code was also tested again using a different half mile section and comparing the results to GDOT's line laser. The results for the 1 mile used to develop the code and the ½-mile test set were all under 10% different from GDOT. The results are shown in Table 5-1. MP 95-94.5 is the test set. More data would have been helpful to further confirm the code, but it was not possible to locate another half mile of the 2011 data. The results of this test support the use of the chosen filter and the mean of the percentile.

Table 5-1 – Comparison of half-mile RVD values for GDOT and GaTech

Mile Point	GDOT	GaTech	Difference
95-94.5	2.141	2.326	8.60%
95.5-95	2.092	2.232	6.69%
96-95.5	2.538	2.297	-9.50%

Another consideration for the computation was whether to use just the wheelpath or the entire image for computation. To test this, the RVD was calculated along the 3.5-foot wheelpath on each image as defined by the milled edge drop-offs. The results showed little difference between the two options when compared for median, variance, and skewness. The medians were 0.04 mm different, variance 0.09 mm^2 different, and

skewness 0.1 mm^3 different. Due to the closeness, either could be chosen. The full-width is considered preferable for two reasons. The first is that the milled edge does not necessarily represent the lane-marking location, so the wheelpath location is uncertain. The second is that the measurement is meant to measure the ability of water to flow, which would flow beyond the wheelpath. Therefore, the full-width should be used.

The final output is a matrix of RVD values calculated every 100 mm in the transverse direction and across each profile through the image. A display can be toggled that looks like the one in Figure 5-6. The blues show a low RVD and the reds a high RVD. Note that Figure 5-6 does not have the milled edge removed, resulting in the high RVD values in columns 1-6.
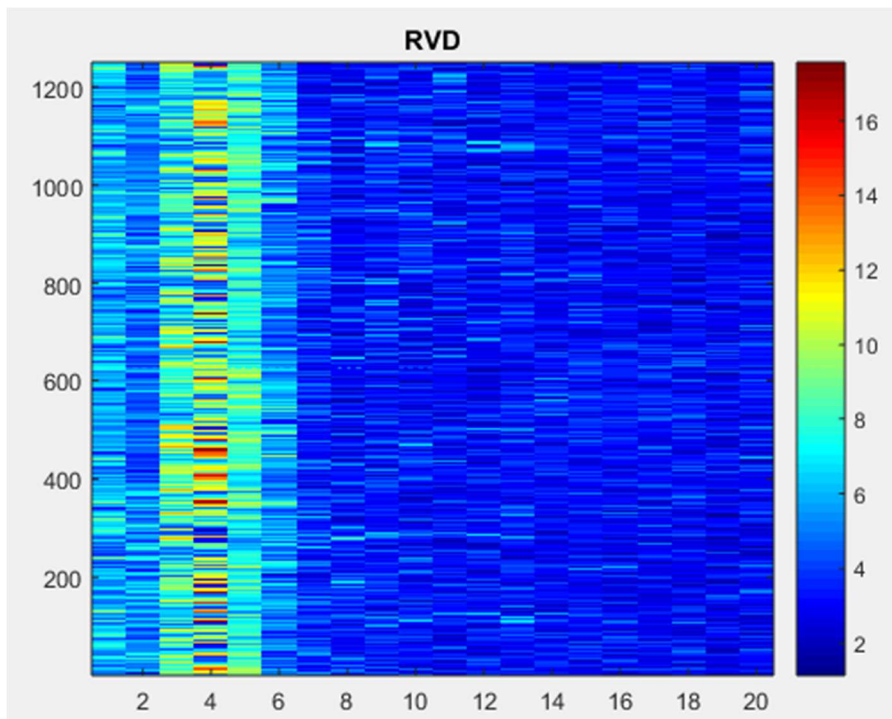
Figure 5-6 – RVD map output

5.1.4   Batch Processing

Once the single image RVD computation was finalized, it was simple to include the option to batch process. The milled edge removal is only used when batch processing. When batch processing, the milled edge details must be included and the first image in the folder chosen. The code will then determine the number of images in the folder and create a vector of file numbers starting with the first image number in the folder. Once an image is opened, it is removed from the vector of file numbers, and the next file number is ready to be chosen after that computation is performed. In this way, the code will iterate through all the images in a folder as long as none of the file numbers are missing.

In addition, some minor changes were needed to make this process more user friendly. A new way of saving the files was created to aid in the ease of manipulating the files. The left and right images are saved separately to avoid overlap causing problems in any later processing. They can be saved as both a CSV and MAT file. Additionally, the ability to toggle the RVD display was added so the user would not need to close hundreds of RVD graphs after batch processing and to speed up the process.

5.1.5   Post-Processing

A post-processing code was written called simply ProcessFiles. This code takes the matrix of RVD values and calculates the median RVD, standard deviation, and skewness, and it can save histograms for each image. This aids in a more aggregated final analysis of the data. The output is a CSV file containing the results in this order from the first row: image number, left image median, left image variance, left image skewness, right image median, right image variance, right image skewness.

5.2   Example Computation

An example of the RVD computation for the first image of the I-95 data is presented here. It will be discussed as if the code would continue to batch process the rest of the files, but the computation is the same for each image, so one should be sufficient.

The first image shows a clear milling drop-off on the left image, but it is not as clear on the right image. This can be seen in Figure 5-7. The first step is to determine the limits CSV file with the area to calculate. This can be done using a lane marking detection code. It can also be done using the RVD display.
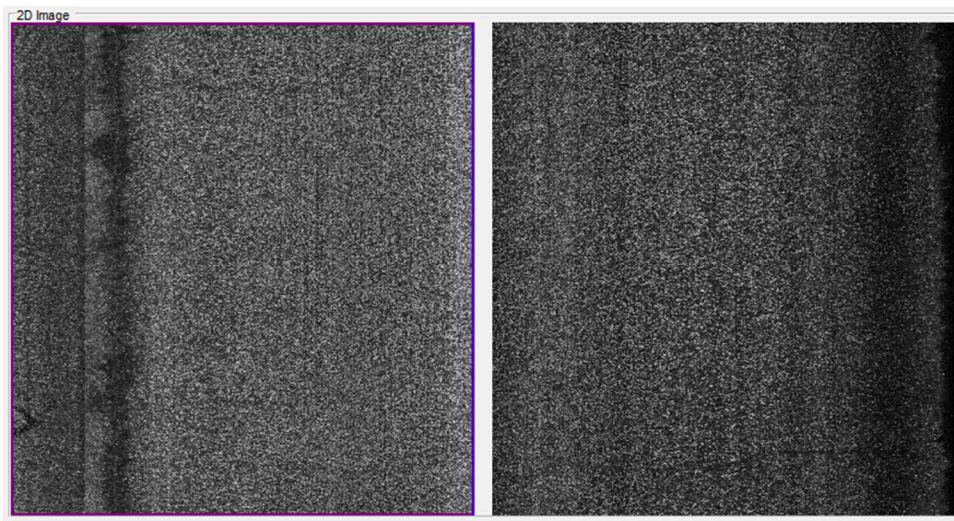
**Figure 5-7 – Image used for this example**

Figure 5-6 is the output for the left image here. The first six columns of RVD readings show abnormally high RVD values, so those can be removed by inputting a limit to the left into the CSV file. For example, since each column is 100 mm wide, removing the left 600 mm could solve this issue. After finding the best one for the first image, it is good to check that this is reasonable for images throughout the section. In this case, it was,

so the CSV file looks like that shown in Figure 5-8. The first column (A) is the left limit; the next (B) is the right limit. The next two columns (C, D) are not needed by this code and could have any values. The fifth column (E) displays the image number. This quality control check must be done using the lane marking detection method, as well.

	A	B	C	D	E
1	600	3780	1	8	315
2	600	3780	1	8	316
3	600	3780	1	8	317
4	600	3780	1	8	318
5	600	3780	1	8	319

Figure 5-8 – CSV file used for showing the limits of RVD computation

After the area selection, the resulting image is more meaningful, and more gradation can be seen. The output after selecting the area is shown in Figure 5-9. The median and standard deviation are displayed in the user interface, as shown in Figure 5-2.
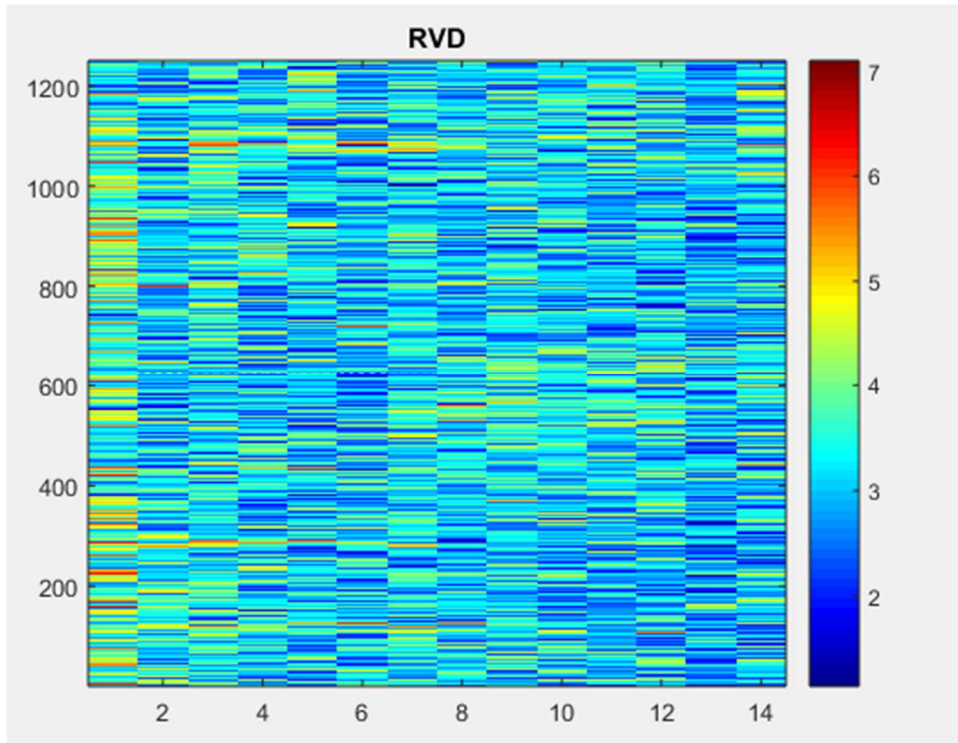
Figure 5-9 – RVD output after area selection

Next, the RVD is calculated for each 100-mm profile. This can be changed using the drop-down menu for the baseline shown in Figure 5-2. The most important portion of the RVD computation code is shown below:

```
for k = 1:m
% find peaks, both high and low
  [pks_max,locs_max] = findpeaks(submat(k,:));
  [pks_min,locs_min] = findpeaks(-submat(k,:));
%find the number of values to take for the top 22%
  lx=floor(.78*length(locs_max));
  ln = floor(.78*length(locs_min));
% sort the peaks from highest to lowest
```

pks_max = sort(pks_max, 'descend');

pks_min = sort(pks_min, 'descend');

%find the minimum and maximum value and save to the matrix maximum and minimum values

maximum = mean(pks_max(1:end-lx));

minimum = mean(pks_min(1:end-ln));

maxmat = [maxmat ; maximum];

minmat = [minmat ; minimum];
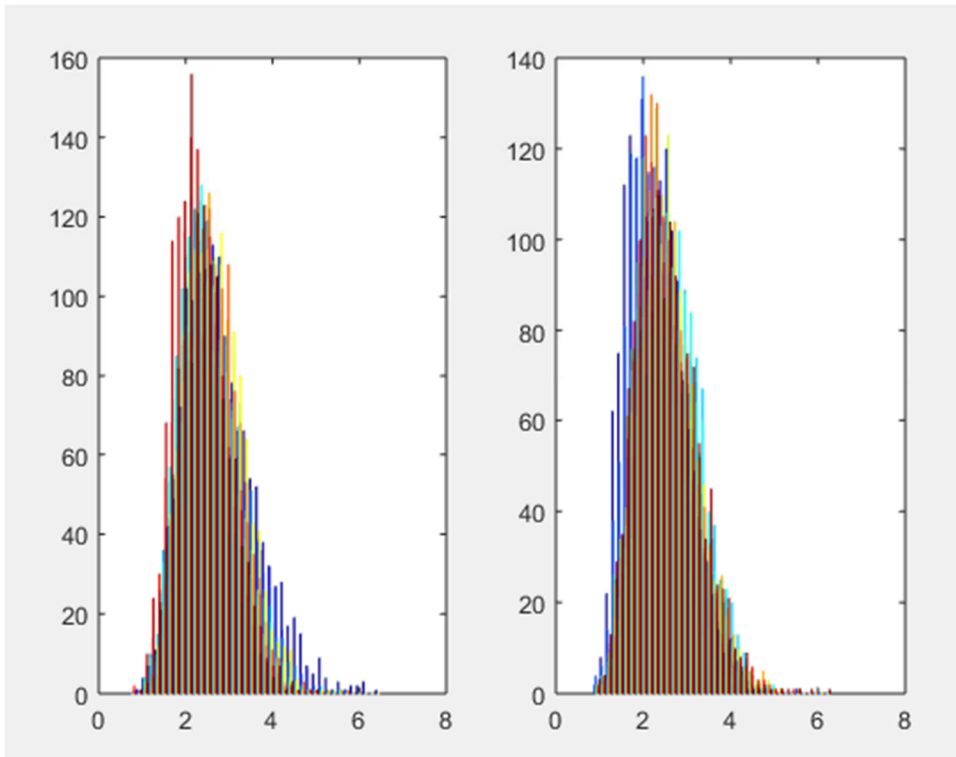
End

%calculate RVD across the matrix

RVD(:,i) = maxmat + minmat;

Submat is a 100-mm-wide column of the image, and this part of the code iterates through the column to calculate the RVD for each row. The findpeaks function is used to determine the maximum and minimum values. The minimum peaks are found by negating the submat input, which makes the most negative value become a high peak. This requires there to be a negative value in the vector, but this seems to always be the case. Next, the locations vector is used to find the number of values to separate to get just the top 22%. The maximum is found using the mean of these top 22% peaks for each. Then they are saved to a matrix. The RVD is calculated using matrix operations (maxmat is the matrix of maximum values for each 100-mm segment; likewise, minmat is the minimums) to reduce the needed loops. Typically, the maximum and minimum would be subtracted, but the minimum value has been negated, so it must be added (by subtracting the negative minimum value). This is iterated through each 100-mm column of the overall area

calculated. This produces a matrix of RVD values, which is saved for each image in the format "RVDMatrix####side.mat" where the #### represents the last 4 numbers of the image number and the side is either left or right.

The next step is to call the ProcessFiles (files,right,left,histogram) function. The inputs for this function are the vector of file numbers, then whether the right and/or left calculation is desired. Using a 1 means that the side should be calculated. A 1 for the histogram input means that the histograms of RVD values for each image should be made; this is always done for both the left and right RVD matrices. For example, ProcessFiles (315:350,1,0,1) would calculate the parameters for files 315-350 for the right-side images and save the histograms for both the left and right images for files 315-350. This saves files of histograms named "histogram-####.fig" with the #### representing the last four digits of the image number. An example of a saved histogram is given in Figure 5-10. The colors have no meaning and are just how Matlab® plots. Figure 5-11 is a screenshot of some of the output table from ProcessFiles called "processedresults.csv". As mentioned, the rows are 1: image number, 2: left median, 3: left variance, 4: left skewness, 5: right median, 6: right variance, 7: right skewness.

Figure 5-10 – Example of histograms from an RVD file

Figure 5-11 – Screenshot of processedresults.csv

These outputs can be manipulated to get many different parameters about the roadway. Some of the initial findings using this method are described in the next section.

5.3   Initial Findings

The batch-processing algorithm was used to analyze the RVD along an approximately one-mile segment on I-95 from the micro-milling project in 2011. This is the only project with 3D sensing data on the micro-milled surface. Mile 95-94 in the southbound direction was chosen because it had half the section with little distress on the surface in 2016 and half with the most distress on the surface along the project in 2016. The half with the most distress of the project, in fact the only section with cracking reported in GDOT's PACES, starts right after a construction joint, so it is possible that the difference in performance can be attributed to a difference in construction.

The analysis was performed in two directions to limit bias from one aspect. One way the analysis was performed was by looking at images/sections of images with the RVDs above 3.2 in 2011 and observing their performance in 2016 to see if the high RVDs correlated with poor performance. The other direction looked at the poorly performing areas in 2016 and observed the RVDs in 2011. In addition to the two directions, several measurements of the RVD were considered. The three considered were the median RVD value, standard deviation, and skewness. The standard deviation showed no correlation to the performance, but the median RVD and skewness will be discussed in this section. The median isn't as impacted by outliers, which is why it is used here.

Looking at the median RVD, there were 12 images with an RVD over 3.2 mm. These images were clustered at the beginning of the section with only 1 image in the latter half. As discussed previously, no cracks were reflected in the beginning half of the section. This hints that cracking may not be correlated to RVD values. To further check this, the

RVD of heavily-cracked sections was considered. These sections did not show a high RVD. For example, this crack, shown in Chapter 2 and here in Figure 5-13a, only resulted in an RVD of 2.2 mm. Further, the length of propagated cracking aggregated at 10 m was compared to the RVD averaged over 10 m, and the resulting graph is shown in Figure 5-12. As can be seen, the segments with no cracking ranged from an RVD of approximately 1.5-3.5 mm. The few sections with cracking were clustered around an RVD of 2-2.7, but having so few sections with cracking and so many more with similar RVD values and no cracking further supports that RVD and cracking are not correlated. Future studies when there is more cracking are needed to confirm this, as it seems cracking may be associated with RVDs in the range of 2-2.7 mm.
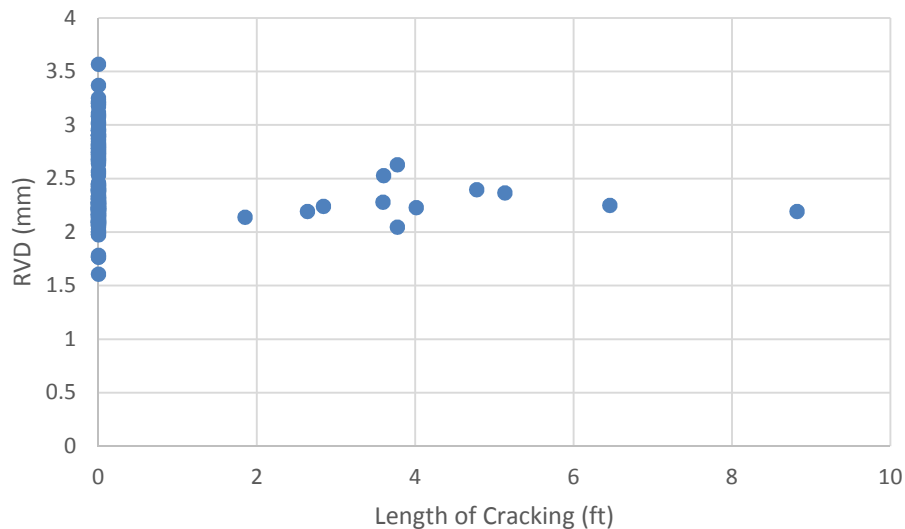
Figure 5-12 – Comparison of RVD with cracking length

Looking again at the image in Figure 5-13a, although the RVD was low, the skewness was interesting. The more severe the cracking in an image, the higher the skewness. For example, for this image, the skewness is 2.4 mm^3, but the average skewness

for the mile is 0.9 mm^3. The histogram is given in Figure 5-13b and shows the positive

skew and the tail in the higher range from the cracking. The skewness relating to cracking

seems logical, as the RVD along the crack is high, but over the image, it is a small area that

would only have a minor impact on the median.

(a)   (b)
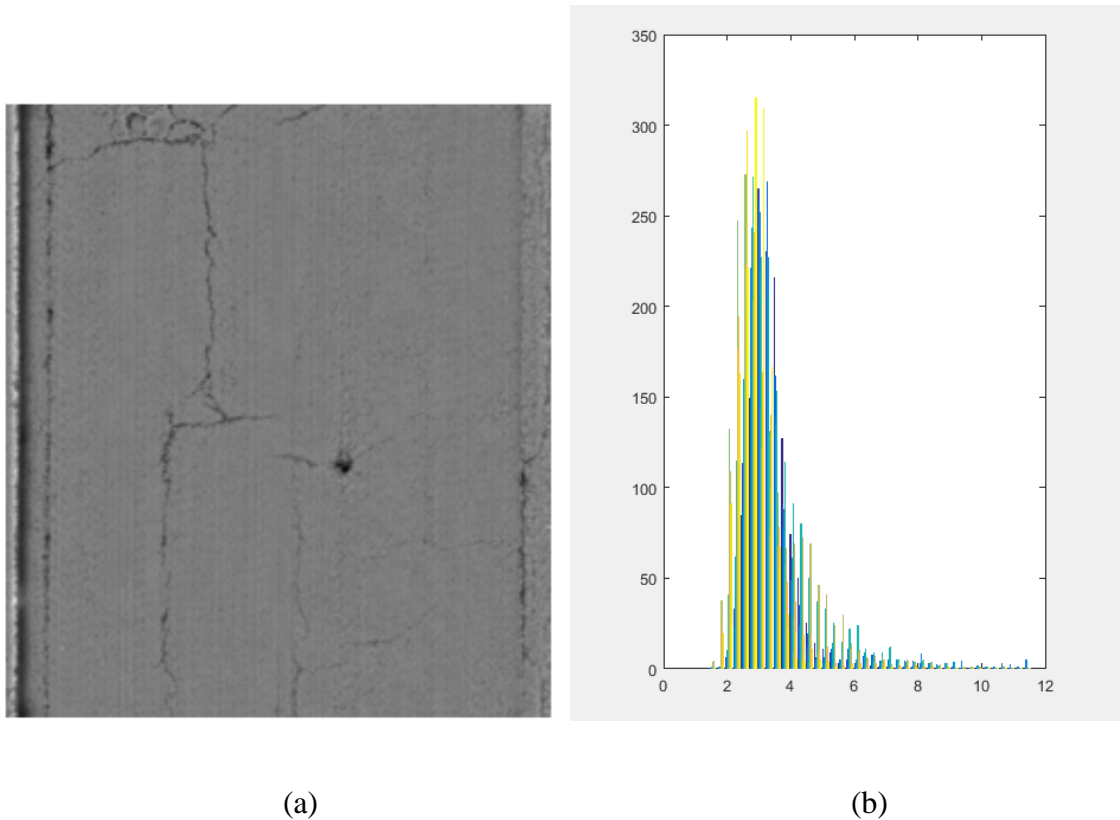
**Figure 5-13 – a) intensity image with bad cracking b) histogram for this image, x axis
is RVD values**

The raveling per image was also considered, but the severity of raveling is still very

low with only one image with Severity Level 1 raveling. The spatial distribution of the

raveling was considered along with the spatial distribution of the high RVD values. There

were 4 major clusters of raveling. The median RVDs that matched the clusters however,

were not any higher than the sections without raveling. The raveling severity was found by

averaging 6 raveling severity readings per image. Most of the raveling clusters showed raveling at a level of 0.5 or less. There was one section of the first cluster with many readings above 0.5, and 10 of the RVD readings above 3.2 mm were within this sub-cluster of higher severity raveling. More raveling may be needed to really determine the relationship between RVD and future raveling, but this suggests that high RVD can contribute to raveling in the future. It is recommended that this study be continued in the future when more raveling has occurred to see how higher RVD impacts raveling in terms of both time to start and spatially. This could give further insight into whether 3.2 mm is the best choice of limit. At this point, it seems to be a reasonable value.

5.4 Summary

This section detailed how the automatic computation of RVD was performed and why it is performed that way. Further improvements to the code could improve the speed, combine the right and left images so the overlap is not a concern, and improve user friendliness. The code is currently capable of producing RVD results similar to those obtained by the GDOT point laser, which is considered the goal, so the code is considered accurate for measuring RVD.

This section also described the method and some initial results of the analysis of RVD's current standard. With only a half-mile segment showing distress, the sample size was too small to determine anything with confidence. However, the initial findings show that the 3.2 mm median value does not have an impact on crack propagation, but it may have some impact on raveling when the RVD is above 3.2 mm. The standard deviation showed no correlation, but the skewness showed some correlation to cracking on a milled surface. The

sections with a lot of cracking had more highly-skewed distributions, as expected. Overall, it was not possible to say with confidence whether the 3.2 mm 50th percentile RVD requirement is the best choice of value, but it shows no evidence to be ineffective at this point.

CHAPTER 6.   CONCLUSION AND RECOMMENDATIONS

6.1   Summary of Contributions

This thesis assesses the sustainability of a new pavement preservation treatment, micro-milling and thin overlay, and improves a method of automatically measuring the primary quality control measure. The main contributions of this thesis include the following:

- A review of how micro-milling is used in the United States

- Performance assessment of the method that showed micro-milling and thin overlay:

    o has an expected service interval of 10-12 years, the same as conventional milling

    o may be a good crack relief treatment, as evidenced by only 5% of cracking reflecting in 5 years on I-95

    o can ameliorate rutting for a short time (approximately 4 years)

- LCCA showing that micro-milling and thin overlay can save 53% the cost of conventional milling. This is a savings of $6,560 per lane-mile per year over the lifetime. If used on all the asphalt interstates in Georgia, it could save over $500 million per year.

- A break-even analysis showing that the treatment must last 5 years to have the same life cycle cost as conventional milling

    o This was somewhat sensitive to the cost of micro-milling; a sensitivity study showed the break-even life being 8 years if the same price difference as that

of the first micro-milling project is employed. This is still below the service interval.

- LCA demonstrating that micro-milling and thin overlay produces 61.7% percent fewer greenhouse gases, uses 61.8% percent less water, and uses 61.9% percent less energy

  o These values were sensitive to RAP use, so using as much RAP as possible in pavement construction is recommended

- A qualitative review of social impacts, such as the reduced construction time and increased flexibility that improves the safety of drivers and workers

- A refined code for calculating RVD, which has been tied to ground truth and is capable of batch processing

- A preliminary study of RVD showing a procedure for future studies, that RVD does not impact cracking, and that the current standard is producing good performance

Collectively, these contributions will aid decision-makers through the quantification of the performance and sustainability of the method. Further, the code will aid those interested in implementing the method. These results could be used to support and aid in the development of a national standard for this treatment, which has been shown to be effective and sustainable compared to the previous standard practice.

6.2   Recommendations

The following lists recommendations for future work:

- Extend performance analysis once more projects are nearing the end of their service interval

- Study what pre-conditions make a project a candidate for micro-milling and the necessary pretreatments for micro-milling using more projects

- Include user costs and traffic control in LCCA

- Refine LCA with data from the actual construction equipment, especially between milling machines to test how milling intensity and speed impact fuel consumption

- Adjust LCA to include OGFC and SMA because they use specialized binders and aggregate that may not be currently represented by PaLATE

- Use an LCA model that is more flexible and can represent the difference in construction flow and timing between the methods and the other minute differences between the two methods

- Quantify the social results, including modeling the queue formed from construction traffic

- Add an automatic edge drop-off detection to the RVD code

- Transfer the code to another language that will enable it to run faster. When doing so, separate the RVD code from the faulting code, as RVD is only measured on asphalt pavement and faulting on concrete pavement

- Develop a national standard for micro-milling and thin overlay, an effective and sustainable pavement preservation treatment

REFERENCES

1. Alternative Fuels Data Center: Maps and Data - Annual Vehicle Miles Traveled in the U.S. https://www.afdc.energy.gov/data/10315. Accessed Aug. 30, 2017.

2. FHWA. MAP-21 | Federal Highway Administration. https://www.fhwa.dot.gov/map21/. Accessed Aug. 30, 2017.

3. FHWA. Fixing America's Surface Transportation Act or the FAST Act - FHWA | Federal Highway Administration. https://www.fhwa.dot.gov/fastact/. Accessed Aug. 30, 2017.

4. FHWA. *FHWA Forecasts of Vehicle Miles Traveled (VMT): Spring 2017*. 2017.

5. ASCE. 2017 Infrastructure Report Card: Roads. https://www.infrastructurereportcard.org/wp-content/uploads/2017/01/Roads-Final.pdf. Accessed Aug. 28, 2017.

6. Pavement Interactive. Micro-Milling – The Finer Side of Milling | Pavement Interactive. http://www.pavementinteractive.org/2011/09/20/micro-milling-the-finer-side-of-milling/. Accessed Nov. 6, 2017.

7. Latham, A. MICRO MILLING Applications and Advantages for Pavement Preservation.

8. Dan Brown. Fine-Mill Pavements for Smooth Thin Overlays - TSP2. *Pavement Preservation Journal*, 2012.

9. Asphalt Forum Responses. Vol. 25, No. 1, , 2013.

10. For Construction Pros.com. When More Teeth Make Quick Work: Micromilling Is Used to Remove Shallow Ruts on Nebraska's Interstate Pavements. *For Construction Pros.com.* http://www.forconstructionpros.com/pavement-maintenance/preservation-maintenance/article/10288520/when-more-teeth-make-quick-work. Accessed Aug. 25, 2017.

11. Cook, M. C., S. B. Seeds, H. Zhou, and R. G. Hicks. Guide for Investigating and Remediating Distress in Flexible Pavements California Department of Transportation's New Procedure. *Transportation Research Record: Journal of the Transportation Research Board*, Vol. 1896, 2004. https://doi.org/10.3141/1896-15.

12. How Micromilling Is Saving States Money on Asphalt Road Repairs. *for construction pros.* http://www.forconstructionpros.com/pavement-maintenance/preservation-maintenance/article/10456001/how-micromilling-is-

13. Merritt, D. K., C. A. Lyon, and B. N. Persaud. *Evaluation of Pavement Safety Performance , February 2015 - FHWA-HRT-14-065*. 2013.

14. Kline, L. COMPARISION OF OPEN GRADED FRICTION COURSE MIX DESIGN METHODS CURRENTLY USED IN THE UNITED STATES.

15. Tsai, Y., Y.-C. Wu, A. Gadsby, and S. Hines. Critical Assessment of the Long-Term Performance and Cost-Effectiveness of a New Pavement Preservation Method: Micromilling and Thin Overlay. *Transportation Research Record: Journal of the Transportation Research Board*, No. 2550, 2016, pp. 8–14.

https://doi.org/10.3141/2550-02.

16.   Tsai, Y. J. Personal Correspondence.

17.   Traffic Counts in Georgia. http://geocounts.com/gdot/. Accessed Aug. 31, 2017.

18.   Lai, J., M. Bruce, D. M. Jared, P. Y. Wu, and S. Hines. Georgia's Evaluation of
        Surface Texture, Interface Characteristics, and Smoothness Profile of Micromilled
        Surface. *TRB 2009 Annual Meeting CD-ROM*, 2009.

19.   Tsai, Y., Y. Wu, and Z. Lewis. Full-Lane Coverage Micromilling Pavement-Surface
        Quality Control Using Emerging 3D Line Laser Imaging Technology. *Journal of
        Transportation Engineering*, Vol. 140, No. 2, 2013, p. 4013006.
        https://doi.org/10.1061/(ASCE)TE.1943-5436.0000604.

20.   Lai, J., S. Hines, P. Y. Wu, and D. M. Jared. Pavement Preservation with
        Micromilling in Georgia: Follow-Up Study. *Transportation Research Record
        Journal of the Transportation Research Board Transportation Research Board of
        the National Academies*, No. 2292, 2012, pp. 81–87. https://doi.org/10.3141/2292-
        10.

21.   Tsai, Y., Y. Wu, J. Lai, and G. Geary. Ridge-to-Valley Depth Measured with Road
        Profiler to Control Micromilled Pavement Textures for Super-Thin Resurfacing on
        I-95. *Transportation Research Record Journal of the Transportation Research
        Board Transportation Research Board of the National Academies*, No. 2306, 2012,
        pp. 144–150. https://doi.org/10.3141/2306-17.

22. ASTM. *ASTME1845 Standard Practice for Calculating Pavement Macrotexture Mean Profile Depth.* .

23. Tsai, Y. A Sustainable and Cost-Effective Pavement Preservation Method: Micro-Milling and Thin Overlay. *Journal of Transportation Engineering*, 2015.

24. GDOT. *Department of Transportation State of Georgia Special Provision Section 432*. 2009.

25. ASCE. *Policy Statement 418 The Role of the Civil Engineer in Sustainable Development*. 2016.

26. Tsai, Y. J., and A. Gadsby. PRELIMINARY LIFE CYCLE ASSESSMENT OF A NEW AND COST EFFECTIVE PAVEMENT PRESERVATION TREATMENT : MICRO-MILLING AND THIN OVERLAY. pp. 1–6.

27. GDOT. PACES Manual. 2011.

28. Geary, G. Personal Correspondence. 2017.

29. Curran, M. A. Life Cycle Assessment: Principles and Practice. 2006.

30. Fhwa. *Pavement Life Cycle Assessment Framework*. 2016.

31. Sukin, G. Petroleum Extraction: More Than Just a Trip to the Gas Tank. *RTSCorp*. http://www.rts-corp.com/industry-bits/bid/176378/Petroleum-Extraction-More-Than-Just-a-Trip-to-the-Gas-Tank. Accessed Sep. 4, 2017.

32. Asphalt Production and Oil Refining | Pavement Interactive. *Pavement Interactive*.

http://www.pavementinteractive.org/asphalt-production-and-oil-refining/.

Accessed Sep. 4, 2017.

33. Whiteside, G. G. How Asphalt Cement Is Made - Material, Used, Processing, Components, Dimensions, Product, Industry, Machine. http://www.madehow.com/Volume-2/Asphalt-Cement.html. Accessed Sep. 4, 2017.

34. Aggregate | Pavement Interactive. *Pavement Interactive*. http://www.pavementinteractive.org/aggregate/. Accessed Sep. 4, 2017.

35. Barnes, L. Personal Correspondence.

36. *Approval of Recycled Asphalt Pavement (RAP) for Use in Asphalt Mixtures*. SOP 41, 2014.

37. Norouzi, A., Y. R. Kim, S. S. Kim, and J. Yang. Effect of Reclaimed Asphalt Pavement Content and Binder Grade on Fatigue-Resisting Performance of Asphalt Mixtures in Georgia. *Journal of Materials in Civil Engineering*, Vol. 29, No. 9, 2017, p. 4017115. https://doi.org/10.1061/(ASCE)MT.1943-5533.0001960.

38. Nathman, R. K. PaLATE User Guide, Example Exercise, and Contextual Discussion. 2008.

39. Nathman, R., S. McNeil, and T. Van Dam. Integrating Environmental Perspectives into Pavement Management. *Transportation Research Record: Journal of the Transportation Research Board*, Vol. 2093, 2009, pp. 40–49.

https://doi.org/10.3141/2093-05.

40.   Chester, M., A. Horvath, and S. Madanat. Parking Infrastructure: Energy, Emissions, and Automobile Life-Cycle Environmental Accounting. *Environmental Research Letters*, Vol. 5, No. 3, 2010, p. 34001. https://doi.org/10.1088/1748-9326/5/3/034001.

41.   Chan, S., B. Lane, T. Kazmierowski, and W. Lee. Pavement Preservation A Solution for Sustainability. *Transportation Research Record: Journal of the Transportation Research Board*, Vol. 2235, 2011, pp. 36–42. https://doi.org/10.3141/2235-05.

42.   Cross, S. A., W. H. Chesner, H. G. Justus, and E. R. Kearney. Life-Cycle Environmental Analysis for Evaluation of Pavement Rehabilitation Options. *Transportation Research Record: Journal of the Transportation Research Board*, No. 2227, 2011.

43.   Alkins, A., B. Lane, and T. Kazmierowski. Sustainable Pavements: Environmental, Economic, and Social Benefits of In Situ Pavement Recycling. *Transportation Research Record: Journal of the Transportation Research Board*, Vol. 2084, 2008, pp. 100–103. https://doi.org/10.3141/2084-11.

44.   Section 828—Hot Mix Asphaltic Concrete Mixtures 828.1 General Description 828.2 Materials Section 828—Hot Mix Asphaltic Concrete Mixtures.

45.   Astec. The Double Barrel Combination Aggregate Dryer/Drum Mixer. https://www.astecinc.com/images/file/literature/Astec-Double-Barrel-EN.pdf. Accessed Oct. 6, 2017.